THE BENEFICIAL REUSE OF ASPHALT SHINGLES IN ROADWAY CONSTRUCTION

by

Tuncer B. Edil and Justin D. Warner

Final report submitted to the
Solid Waste Reduction and Recycling Demonstration Program
Wisconsin Department of Natural Resources

Project 6-13

Geo Engineering Consulting LLC

November 30, 2007

EXECUTIVE SUMMARY

Approximately 11 million tons of reclaimed asphalt shingles (RAS) are disposed in landfills every year. Research has demonstrated that these materials can be recycled into a variety of products. A widespread, large-scale recycling and reuse application would utilize an otherwise wasted resource while clearing landfill space and creating new business opportunities.

One potential reuse application is the utilization of RAS in the aggregate base (AB) and subbase (ASB) layers of roadway pavements and as working platforms for pavement construction over soft subgrades, and as embankment fills. RAS has the potential to act as an additive or substitute for the earth materials typically utilized in these applications. Like any recycling activity, the proper regulatory and permitting requirements for the reuse of RAS must be addressed. The purpose of this study was to determine the technical specifications of RAS, the effect of fly ash stabilization on RAS strength, and the practicality of the widespread implementation of RAS in roadway applications. RAS, fly ash stabilized RAS (S-RAS), RAS-aggregate mixtures, and RAS-silt mixtures were evaluated for particle size characteristics, compaction characteristics, California Bearing Ratio (CBR), unconfined compressive strength, and resilient modulus.

In summary, RAS is a granular material with particle size characteristics similar to that of well-graded sand, however, with very different particle shape and strength. RAS stiffness, in general, increases with increasing dry unit weight, and RAS dry unit weight increases with decreasing maximum particle size and increasing fines percentage; although the nature of RAS particles also play a role. The localized penetrative resistance, or CBR, of RAS is small.

According to resilient modulus test results, pure, chemically unstabilized RAS is unsuitable as base material although unstabilized RAS can be used as subbase or general fill material (resilient modulus ~ 30 MPa). Additionally, RAS-Grade 2 granular backfill mixtures (minimum 50:50 mass-to-mass ratio) are suitable for use as subbase and are potentially suitable for use as base course in an unstabilized state (resilient modulus ~ 77 MPa). Mixtures of RAS with Grade 2 granular backfill exhibit decreasing stiffness with increasing RAS content.

Fly ash stabilized (class C fly ash at 20% by dry mass of RAS) RAS (S-RAS) is less susceptible to penetrative deformation than unstabilized RAS, however; S-RAS is still highly susceptible to penetrative deformation when unpaved. S-RAS experienced measurable improvement in resilient modulus over unstabilized specimens; however, the improvement does not render S-RAS as a base course material (resilient modulus ~ 60 MPa, unconfined compressive strength ~ 200 kPa). S-RAS resilient modulus increases with increased curing length for time periods longer than 7 days, however; overall stiffness gain is small (2-4 MPa). The waste shingles exhibit decreased pozzolanic and cementation activity as compared to other fly-ash stabilized materials. However, other forms of stabilization i.e. cold asphalt emulsion, etc. might prove more effective in strengthening RAS.

Additional studies are necessary to further assess the practicality of using RAS, S-RAS, and RAS composite mixtures as a replacement for virgin aggregates in roadway construction. Large-scale field studies of RAS would be most beneficial. Additional studies are also needed to evaluate other geotechnical applications such as fill, filter or drainage material.

TABLE OF CONTENTS

SECTION ONE

INTRODUCTION

Approximately 11 million tons of reclaimed asphalt shingles (RAS) (Fig. 1(a)) are disposed in landfills every year (Shingle Recycling Organization, 2005). Re-roofing jobs account for 10 million tons (referred as "tear-offs"), with another 1 million from manufacturing scrap. Research has demonstrated that these materials can be recycled into a variety of products (Fig. 1 (b)). Currently, RAS is used primarily as an additive to hot-mix asphalt, however; this application constitutes a small percentage of the total disposed shingles. A widespread, large-scale recycling and reuse operation would utilize the remainder of an otherwise wasted resource while clearing landfill space and creating new business opportunities.

One potential reuse application is the utilization of RAS in the aggregate base (AB) and subbase (ASB) layers of roadway pavements and as working platforms for pavement construction over soft subgrades and embankment fills. RAS has the potential to act as an additive or substitute for the earth materials typically utilized in these applications. Recycled materials such as reclaimed pavement material, reclaimed asphalt pavement, glass, and fiberglass are already used in roadway pavement structures. The addition of RAS to this selection would offer opportunities for additional diversion of waste materials that would otherwise be landfilled.

The biggest impediment to the successful reuse of RAS in roadway applications is the lack of knowledge regarding recycling and re-processing protocol. There is, however; ample information regarding the regional availability of RAS for recycling applications. In a 2003 study characterizing the statewide distribution of municipal solid

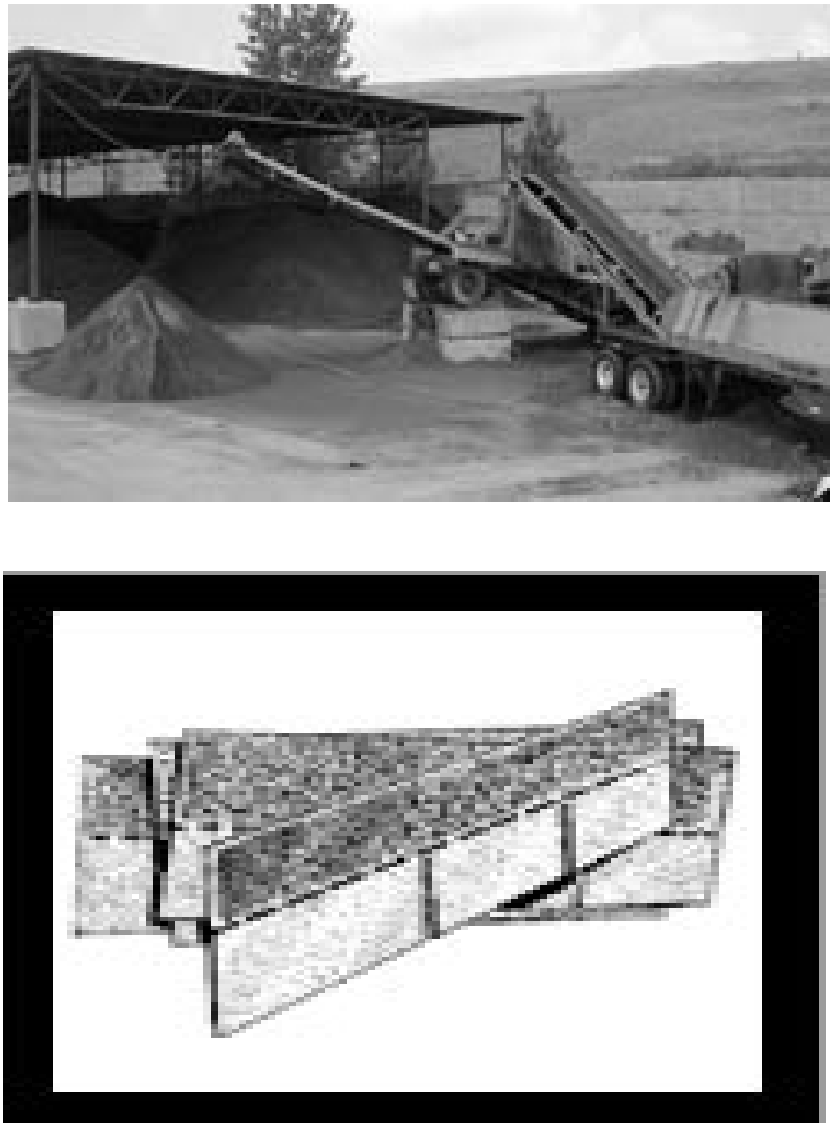

Figure 1.1 Photograph of (a) shingles being ground for reclamation and, (b) shingle tabs prior to roof placement
(Shingle Recycling Organization, 2005)

waste in Wisconsin, the Cascadia Consulting Group estimated that 285,000 tons of asphalt roof shingles were disposed annually in Wisconsin landfills.

Disposed shingles comprise 6% of the total municipal solid waste. As such, shingles constitute the third largest item by weight found in the waste characterization study. The 2003 figure does not include the shingles disposed in construction and demolition waste landfills. The Cascadia Group estimated that construction and demolition debris (~ 30% of materials landfilled) exist in sufficient quantity to offer significant opportunities for additional diversion and recycling of shingle waste.

Like any recycling activity, the proper regulatory and permitting requirements for the reuse of RAS must be addressed. The purpose of this study was to determine the technical specifications of RAS, the effect of fly ash stabilization on RAS strength, and the practicality of the widespread implementation of RAS in roadway applications. RAS, fly ash stabilized RAS (S-RAS), RAS-aggregate mixtures, and RAS-silt mixtures were evaluated for particle size characteristics, compaction characteristics, California Bearing Ratio (CBR), unconfined compressive strength, and resilient modulus.

The results of the completed study are presented. Section 2 provides background information on the following: pavement design and failure criterion, CBR and factors that affect CBR, resilient modulus and factors that affect resilient modulus, unconfined compressive strength and factors that affect unconfined compressive strength. Section 3 describes the materials utilized in the laboratory testing program. Experimental and data analysis procedures are presented in Section 4. A summary and analysis of the test results is presented in Section 5. Final conclusions are presented in Section 6. Section 7 discusses the practical implications of the beneficial reuse of RAS in roadway applications.

SECTION TWO

BACKGROUND

2.1 THE BENEFICIAL REUSE OF RECLAIMED ASPHALT SHINGLES

Currently, RAS is utilized primarily as an additive in hot-mix asphalt (HMA). Several state departments of transportation, including the Minnesota Department of Transportation (MNDOT), have implemented guidelines for the beneficial reuse of RAS in HMA. The guidelines put in place by MNDOT were developed through an extensive study conducted by the department. MNDOT initiated original research and development programs for the recycling and reuse of waste shingles as early as 1990. These investigations were supported by the Recycled Materials Resource Center (RMRC).

The projects focused on field-testing, market development and technology transfer of RAS as an additive in HMA. The projects also addressed the potential applications of RAS as a dust control supplement, and as an unbound aggregate supplement in base course construction, however; the primary objective was to develop guidelines for the addition of RAS into HMA. The research initiative concluded that HMA produced with 5% RAS maintained the bituminous engineering pavement properties essential to quality performance (Crivit, 2005).

Although MNDOT was successful in developing guidelines for the reuse of RAS in HMA, there was still a need for continued research and development in the applications of RAS as a dust control supplement, and additive to virgin aggregates in roadway construction. MNDOT began preliminary research for the development of secondary RAS applications (Crivit, 2005).

In the preliminary analysis, MNDOT identified several barriers to the successful implementation of the wide-spread reuse of RAS in roadway construction applications (dust inhibitor, and additive to virgin aggregates). First, there is a general lack of specifications and end-use demand for RAS in roadway applications. Second, the supply of RAS is limited. RAS is currently being reused as a 5% additive in HMA and there is sufficient source material for this application, however; an additional reuse initiative would heighten the demand for RAS and may deplete the current supply. Third, there is a lack of communication and outreach in regards to the technical, economic, and environmental benefits of shingle-derived products (Crivit, 2005).

In order to address the aforementioned challenges, MNDOT oversaw several independent research projects designed to assess the technical, environmental, and economical feasibility of RAS in roadway construction. In November, 2001, MNDOT oversaw a demonstration by Bituminous Roadways Inc., and SKB Environmental on the utilization of RAS cold-blended with virgin aggregates as a dust control measure. The RAS was blended at a 50:50 volume-to-volume ratio and compacted to specified density. Researchers working on a similar project for the Iowa DOT found that RAS tended to bind the aggregate and minimized dust in a construction environment (Marks and Petermier, 1997).

Additionally, the MNDOT in conjunction with RMRC, oversaw field tests of RAS blended with a traditional unbound aggregate for use as base course. The purpose of the study was to observe and quantify the performance of a Class 7 – BC (as defined by MNDOT specifications) aggregate containing a maximum of 10% RAS by volume. The project is underway, but has not yet been completed. At this time, only qualitative observations have been made in regards to RAS performance as an aggregate additive (Crivit, 2005).

Other state DOTs have undertaken projects similar to those initiated by MNDOT, and many of these studies have indicated that RAS has a beneficial effect on some soils, but again; these observations were largely qualitative. Hooper and Marr (2004) cited the lack of quantitative evidence and sought to provide baseline quantitative data regarding the performance of RAS and RAS composite mixtures as base course.. Hooper and Marr performed sieve analyses, Atterberg limits, modified Proctor compaction tests, and CBR tests on 25-mm minus RAS mixed with increasing amounts (0, 33, 50, 67 and 100% by volume) of crushed stone gravel. They also tested 25-mm minus RAS blended (33% by volume) with either a silty sand, a clean sand, or clay. The RAS used in this study was developed exclusively from pre-consumer, off-specification shingles obtained directly from shingle manufacturers. Although the RAS in this study was composed entirely of manufacturer scrap shingles, the authors expected the results to apply equally well to post-consumer, tear-off shingles provided wood, nails, plastic, and other residue material are removed prior to processing.

Hooper and Marr (2004) found that the CBR of the crushed stone gravel was 92% prior to RAS addition. CBR of 25-mm minus RAS was 6%. The addition of RAS at the specified intervals resulted in a diminishment in CBR of the crushed stone gravel. A summary of the CBR results from Hooper and Marr's study of RAS blended with crushed stone gravel are shown in Table 2.1.

Hooper and Marr (2004) found that CBR of the silty sand was 33%, CBR of the clean sand was 21%, and CBR of clay was 8% prior to RAS addition. The addition of RAS resulted in a decrease in CBR for the silty sand and clean sand, but resulted in an increase in CBR for clay. A summary of the CBR results from Hooper and Marr's study of RAS blended with a silty sand, a clean sand, and a clay are shown in Table 2.2.

Table 2.1 1CBR of RAS and RAS-crushed stone gravel blends (after Hooper and Marr, 2004)

Material	Compaction Dry Unit Weight (kN/m^3)	Compaction Water Content (%)	Plasticity Index	CBR
25-mm minus RAS (100%)	13.7	8	NP	6
Crushed Stone Gravel (100%)	19	7	NP	92
67:33 CSG:RAS	16.5	11	NP	23
50:50 CSG:RAS	16.2	9	NP	20
33:67 CSG:RAS	15.1	11	NP	20

Note: NP = non-plastic

In conclusion, Hooper and Marr found that the addition of RAS to inherently strong materials such as crushed gravel and sand resulted in a decrease in CBR strength. The addition of RAS to inherently weak, plastic materials such as clay resulted in an increase in CBR strength. The authors suspected that where the highly angular particles of gravel and sand contributed to increased interparticle friction, the addition of RAS disrupts this phenomenon and thereby decreases material strength. Even so, the CBR results suggested that RAS-stone gravel blends can be used as a structural fill material and also potentially provide subbase support for pavements and light structures. The authors also suggested that when RAS is added to clay, the cohesion of the clay particles holds the RAS particles in place such that they do not "slip" as easily during CBR testing. Additionally, the introduction of RAS increases the amount of granular material in the clay and thereby increases shear strength during CBR loading.

Hooper and Marr did not investigate the influence of particle size on RAS stiffness. Also, the authors did not investigate the effect of cementing agents such as asphalt emulsion and self-cementing fly ash on RAS stiffness. Finally, they did not investigate RAS resilient modulus, a parameter essential for the empirical-mechanistic design of roadway pavement systems, or unconfined compressive strength. As such, future studies are needed to assess RAS performance in resilient modulus and unconfined compressive strength tests, the effect of particle size on RAS stiffness, and the effect of stabilizing agents as a means to improve RAS performance.

Table 2.2 CBR of RAS-silty sand, RAS-clean sand, and RAS-clay blends (after Hooper and Marr, 2004)

Material	Compaction Dry Unit Weight (kN/m^3)	Compaction Water Content (%)	Plasticity Index	CBR
Silty Sand (100%)	16.5	12	NP	33
67:33 Silty Sand:RAS	16.6	9	NP	19
Clean sand (100%)	14.8	11	NP	21
67:33 Clean Sand:RAS	14.9	10	NP	13
Clay (100%)	16.6	12	13	8
67:33 Clay:RAS	16.2	11	12	20

Note: NP = non-plastic

2.2 ROADWAY PAVEMENT SYSTEMS

2.2.1 Flexible, rigid, and aggregate surface pavement systems

Roadway pavement systems are built to provide a smooth riding surface for automobiles. Pavement systems are designed to withstand, for a given lifespan, the stresses imposed by traffic, and the damaging effects of exposure to wind, rain, heat, and cold. Comprehensive pavement design fully incorporates the properties of the supporting subgrade, the base course, any accompanying subbase, and the paved surface course.

Three types of surface courses are used in the United States. They are 1) unpaved aggregate surfaces, 2) rigid pavements, and 3) flexible pavements. The majority of finished roads in the United States are surfaced with aggregate (AASHTO, 1993). The aggregate is placed directly atop a subgrade and may be stabilized with additives. The entirety of the traffic load is supported by the aggregate layer and the subgrade, thus, aggregate surface roads are most common in low-volume, rural areas.

Rigid and flexible pavements are multilayered structures consisting of a concrete or asphalt surface layer underlain by layers of granular base material. They are used primarily in high-volume regions. The actual pavement sits atop a natural cut subgrade or a fill. Rigid pavements use either reinforced or unreinforced Portland Cement Concrete as the surface course. Flexible pavements use hot mixed asphalt (HMA) as the surface course. In order to prevent contamination of the concrete surface course, the utilization of RAS as subbase and base is being proposed solely for flexible pavement systems.

2.2.2 Empirical-Mechanistic Pavement Design

The typical structural layout for a flexible pavement system is shown in Figure 2.1. Stresses and strain from traffic loading decrease with depth in a pavement system. Thus, the deepest layers in the system are constructed with weaker materials i.e. the subgrade material is usually lower in stiffness and strength than the subbase and base course materials. Flexible pavement systems typically require at least a base course layer to effectively distribute loads to the subgrade, however; a subbase layer of intermediate material is often used to increase thickness and provide filtration between the fine-grained subgrade and coarse-grained base course. Base courses and subbases in flexible pavement systems are often constructed using stiffer materials than those used in rigid systems.

The primary goal of pavement structural design is to develop a system that minimizes the buildup of excessive stresses in each constituent layer while balancing the economic demands and spatial limitations of construction. Modern pavement systems will be designed using an empirical-mechanistic process subject to several limiting conditions which include traffic volume, environment, and serviceability.

Traffic volume is defined as the number of vehicles that pass a prescribed section of road over a set period of time. This number is typically converted into an equivalent single axle load (ESAL). Roadway pavements are designed to support the total ESALs estimated for the planned lifespan of the roadway. Roadways that service a greater number of ESALs require a stiffer pavement structure.

Roadway serviceability is the capability of the road surface to accommodate specific vehicle types. Serviceability is reported as a numerical estimate ranging from 1 (failure) to 5 (perfect) (AASHTO, 1993). Serviceability of a roadway usually decreases over the course of its lifespan, therefore; estimates of expected use must be incorporated into the final pavement design

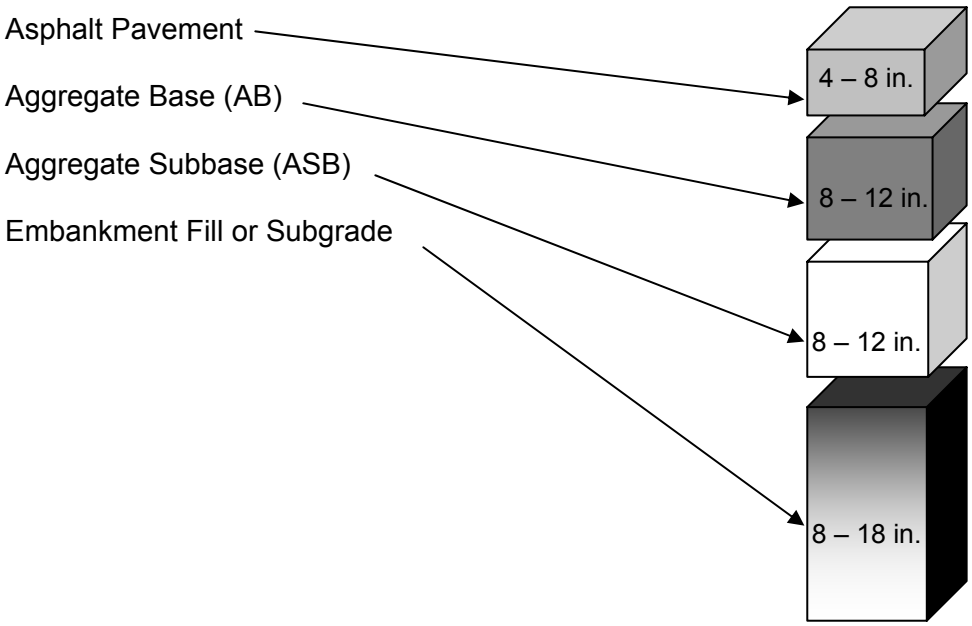

Figure 2.1 Typical structural layout for flexible pavement system

Environmental factors such as subgrade soil and weather greatly affect the long term welfare of roadways. The capacity of subgrade soils to support traffic loads is the greatest influence on the final design depths of the constituent layers in a pavement system (Thompson and Robnett, 1979). Soft subgrade soils are highly susceptible to immediate and often prolonged deformation when loaded, whereas stronger subgrades are more resistant. Pavement strength capacity is also affected by long term exposure to excessive heat, precipitation, and/or freeze-thaw cycles. The overall effect of these and other environmental factors is unique to the pavement's location.

2.2.3 Failure criterion

Pavement design methods are broken into two classes: 1) empirical, and 2) mechanistic. Empirical methods are founded on the correlation between observed pavement performance data and known properties of the pavement structural components. Mechanistic design methods utilize theoretical design concepts in accordance with the known physical properties of the pavement materials (Huang, 1993). The empirical AASHTO method for pavement structural design was first established in 1972 and is the most widely accepted method. The AASHTO method was modified in 1986 to include the dynamic elastic properties of pavement material. The dynamic elastic properties of pavement material are obtainable via resilient modulus, a measurable property of soil (AASHTO, 1993). This modification was considered a major improvement to the overall design of pavement structures.

Pavement failure is defined as the point where deformation of the structural elements is substantial enough to cause an intolerably uneven roadway surface or to cause permanent splitting of the surface layer (Seed et al., 1962). Pavement failure can be characterized by one of two conditions: 1) cracking, and 2) rutting.

Pavement cracking results from structural fatigue, and from thermal effects such as excessive heat exposure and repeated freeze-thaw cycling. Fatigue failure occurs when recurring traffic loads induce the buildup of tensile stresses along the base of the surface layer. As the stress cycles repeat, the permanent strain in the surface layer increases until splitting occurs. The exact number of loading cycles required to produce cracking is dependent on the strength of the pavement structural components (Huang, 1993). The ability of the base course, along with the subbase and the subgrade, to resist cracking is determined by observing material behavior under dynamic loading conditions. Resilient modulus is a numerical quantification of the dynamic elastic properties of road materials. Materials with a high resilient modulus are more resistant to structural fatigue than materials with low resilient modulus.

Pavement rutting, the second type of failure, occurs when the structural components undergo excessive permanent deformation as a result of persistent sub-failure loading. Traffic loading produces a stress and a corresponding strain in the pavement structural components. When this stress is released, the pavement materials rebound, but because these elements are not elastic, some permanent i.e. plastic deformation remains from the loading. Repeated load cycles result in the buildup of plastic strain in the structural layers. Long-term rutting of pavement is a result of the settlement and lateral movement of structural layers that have undergone excessive plastic deformation.

2.2.4 Base course and subbase specifications

Base course is the layer of compacted material beneath the paved surfaces of roadways. Base course is generally composed of aggregate. Aggregate is defined by the Wisconsin DOT (WisDOT) as a composite mixture of hard, durable mineral materials that have been mechanically processed. Aggregate materials are further

classified by gradation, composition, and source. WisDOT uses a grade numbering system to designate different aggregates. The gradation parameters in use by WisDOT are shown in Table 2.3. Grade 2 Granular Backfill is a crushed limestone aggregate commonly used in Wisconsin. Other aggregate materials include pit run, crushed granite, and sand.

Subbase is the layer of compacted material beneath the base course of roadways. The subbase layer is not required by WisDOT, but can be used to provide added support to the base layer and to provide filtration between the course base layer and fine-grained subgrades. WisDOT requires that the maximum diameter of subbase particles shall not exceed ¾ of the compacted thickness of the lift being placed. Additionally, WisDOT requires that at least 25% of the material, by weight, shall pass a No. 4 (4.75 mm) sieve.

Table 2.3 WisDOT grain size parameters for aggregate base course

Sieve Size (mm)	Percentage by Weight Passing					
	Gradation No. 1		Gradation No. 2		Gradation No. 3	
	Crushed Gravel	***Crushed Stone***	***Crushed Gravel***	***Crushed Stone***	***Crushed Gravel***	***Crushed Stone***
37	100	100	100	100	100	100
25	75-100	3/4	100	100	100	100
19	3/4 of previous	3/4 of previous	3/4 of previous	3/4 of previous	95-100	95-100
10	40-75	30-65	50-85	40-75	50-90	50-90
5	30-60	25-55	35-65	25-60	35-70	35-70
2	20-45	15-40	25-50	15-45	20-55	15-55
0.5	10-30	3/4 of previous	10-30	3/4 of previous	10-35	3/4 of previous
0.075	3-10	2-12	3-10	3-12	8-15	5-15

2.3 RESILIENT MODULUS

Resilient modulus is a measure of material stiffness used in empirical-mechanistic pavement design. Resilient modulus is determined through laboratory or in situ testing of HMA, base, subbase, and subgrade materials. Recycled asphalt shingles (RAS), the material of concern for this study was evaluated for resilient modulus to determine total stiffness. The following is a detailed description of resilient modulus in regards to testing protocol, engineering theory, and material variability.

2.3.1 Resilient Modulus Defined

Resilience is the capacity of a material to absorb and release strain energy. The resilience characteristics of a material are determined by applying a series of cyclic, sub-failure loads to a laboratory specimen. Linearly elastic materials will deform under cycling loadings, but will return to their initial dimensions once the load is removed. Linearly elastic materials exhibit no permanent strain, provided that load levels are maintained within the elastic range.

Pavement materials are not elastic materials. Therefore, the concept of resilience must be implemented with caution. When a soil or aggregate is stressed, a strain develops. When the stress is released, a hysteretic behavior is exhibited, i.e. as the applied stress is relieved, the material will begin to rebound, but will never fully rebound to its original dimensions (Mitchell, 1993). The permanent strain left from a loading event is known as plastic strain. Plastic strain is non-recoverable, and accrues with each additional application of stress. The strain that is recovered after a loading event is the resilient strain.

Although the plastic strain experienced by pavement materials exhibits decidedly non-linear behavior, research has shown that the concept of resilience can be applied to these materials in most scenarios (Li and Selig, 1994). Muhanna et al.

(1998) demonstrated that greater than 50% of the total plastic deformation experienced by soils in cyclic loading tests occurs within the first 10 loading cycles. As the number of cycles increases, the incremental change in plastic deformation asymptotically approaches zero and the elastic strain becomes constant. Therefore, resiliency can be measured so long as the measurement is made when the number of loading cycles is sufficient to ensure linearly elastic strain behavior.

Resilient modulus is defined as

$$M_R = \frac{\sigma_d}{\varepsilon_R} \tag{2.1}$$

where M_R is the resilient modulus, σ_d is the deviator stress, and ε_R is the resilient strain (Thompson and Robnett, 1979). Arranged in this manner, the resilient modulus serves as an equivalent to Young's modulus for an elastic material.

2.3.2 Factors That Affect Resilient Modulus

Resilient modulus varies with changes in temperature, water content, gradation, dry density, loading conditions, and the presence or lack of lateral confinement. The following is a discussion of these factors and their effect on soil resilient modulus.

2.3.2.1 Temperature

Resilient modulus of soils is dependent on temperature, but at temperatures above freezing, the effect is minimal compared to factors such as dry density and external loading conditions. In general, lowering the soil temperature will result in an increase in resilient modulus. This effect is attributed to the increase in surface tension in the pore fluid that occurs as temperature is decreased (Jin et al., 1994). The

increased surface tension also results in an increase in soil matric suction which increases interparticle friction.

Soil resilient modulus increases considerably at temperatures below freezing. The frozen pore water binds the soil particles together thereby increasing interparticle friction. However, repeated freeze-thaw cycles can have a negative affect on soil resilient modulus.

Temperature variations can also cause soil resilient modulus to vary seasonally. This is particularly evident in regions that experience large temperature variations between seasons. As such, AASHTO recommends the use of an effective resilient modulus determined as the average of measurements taken on field samples throughout the year (AASHTO, 1993).

2.3.2.2 Density and water content

Density and water content are descriptors used to characterize the physical state of soil or aggregate. Research has shown that soil resilient modulus typically decreases with increasing water content (Thompson and Robnett, 1979). Additional studies have established the existence of a critical saturation level, above which the resilient modulus will drop dramatically. Rada and Witczak (1981) reported the critical saturation level as approximately 80% for typical soils. Resilient modulus reaches a minimum level when soil is completely saturated. The dramatic reduction in resilient modulus is likely due to lowered matric suction at higher water contents (Tian et al., 1998).

Soil resilient modulus increases with increasing dry density. This phenomenon can be attributed to increased particle interaction at higher densities. Thus, increasing compactive energy usually increases resilient modulus (Thompson and Robnett, 1979).

The effect of water content and dry density relative to each other is not fully understood. Research has shown that dry density has a much greater effect on resilient modulus than water content (Thompson and Robnett, 1979). However, some studies have suggested that density does not affect resilient modulus nearly as much as moisture content (Rada and Witczak, 1981).

In light of these findings, the best characterization of soil resilient modulus is one that considers the effect of water content and dry density concurrently (Li and Selig, 1994). At water contents less than optimum, a subsequent decrease in water content without a corresponding decrease in dry density will increase soil resilient modulus. The matric suction in the soil will increase, but without an equivalent drop in dry density, there will no means of balancing the effect that the change in matric suction has on resilient modulus. If the drop in water content is paired with a comparable decrease in density, the resilient modulus will still increase, albeit by a smaller margin because the drop in density serves to offset the increase in matric suction. As noted earlier, some studies have shown that water content has a greater effect on resilient modulus than dry density. In these situations, dry density would have to decrease by a greater margin than the decrease in water content to prevent an increase in resilient modulus.

For water contents greater than optimum, an increase in water content will almost always result in a decrease in resilient modulus. Increasing the water content effectively lowers the matric suction and increases the saturation. Additionally, increases in saturation percentage at water contents greater than optimum almost always correspond to a decrease in density. A decrease in density results in a decrease in resilient modulus. Therefore, resilient modulus will decrease dramatically as a soil is compacted further and further wet of optimum.

2.3.2.4 Particle size, shape and gradation

Resilient modulus is dependent on the particle size characteristics, shape characteristics and fines content of soil. In general, well-graded soils exhibit higher resilient modulus than either poorly-graded or gap-graded soils. Well-graded soils contain a wide range of particle sizes and tend to pack more densely than poorly-graded or gap-graded soils. The increase in density and the heightened influence of interparticle friction increases resilient modulus.

The effect of particle shape on resilient modulus is most pronounced in granular soils i.e. soils with greater than 50% coarse material and aggregates. As angularity increases, so does interparticle friction. For this reason, granular soils with high angularity tend to have higher resilient modulus than soils with sub-rounded to rounded particles (Rada and Witczak, 1981).

Research has shown that resilient modulus decreases with increasing fines content. However, the influence of fines content is specific to soil type (Rada and Witczak, 1981). For instance, resilient modulus is largely unaffected by increases in fine content for coarse, granular soils with high angularity. As maximum particle size and angularity decreases, the effect of fines content on resilient modulus becomes more pronounced. . An Oklahoma DOT study evaluated the resilient modulus of typical well-graded base course gravels at the fine and coarse limits of state specifications. The Oklahoma DOT determined that base material at the coarse limit exhibited resilient modulus approximately 136% higher than base course at the fine limit (Tian et al., 1998).

Resilient modulus also varies with the composition of soil fines. Soils containing low-plasticity fines (low LL and PI) tend to have lower resilient modulus than soils with high-plasticity fines (Thompson and Robnett., 1979). Essentially, soils with mostly silty fines exhibit lower resilient modulus than soils that contain mostly clay fines.

Additionally, organic soils and soils that contain large quantities of particles with low specific gravity (peat, etc.) exhibit low resilient modulus.

2.3.2.5 Lateral confinement

Resilient modulus tends to increase as lateral effective stress is increased. This effect has been exploited in roadway systems through the use of geocells, aluminum grids and other confinement systems. Lateral confinement systems were not utilized in this study, therefore; the effect of lateral confinement on resilient modulus is not directly applicable. Latex membranes are typically used to confine resilient modulus test specimens, however; research has shown that the effect of the latex membrane on resilient modulus is negligible (Edil and Bosscher, 1994).

2.3.2.6 Loading conditions

Of all the factors that affect soil resilient modulus, the loading condition i.e. stress state is by far the most critical. The stress state of soil during resilient modulus testing is defined by the confining pressure and applied cyclic deviator stress.

Confining pressure is defined as the isotropic, principal stress (σ_3) applied to a resilient modulus test specimen. Resilient modulus tends to increase with increasing confining pressure. Deviator stress is defined as the pressure difference between the major principal stresses (σ_1, σ_3). In a resilient modulus test, confining pressure is isotropic such that σ_2 is equal to σ_3. The axial principal stress (σ_1) is equal to the confining pressure plus the applied cyclic vertical stress. Thus, the deviator stress can also be defined as the applied cyclic vertical load over the cross-sectional area of the specimen.

Soils are subjected to a wide range of confining pressures and deviator stresses during a resilient modulus test to determine the overall effect of these variations on

resilient modulus. Specific combinations of confining pressures and deviator stresses have been standardized by AASHTO and the National Cooperative Highway Research Program (NCHRP) to reflect the loading conditions experienced by soils in roadway pavement systems. During a resilient modulus test, a soil is confined with a specified pressure, and subjected to a series of loading "events" or cycles. After the specified number of loading cycles has been completed, the soil is re-pressurized using a higher or lower confining stress and subjected to another series of loading events. The number of loading cycles, and the total number of series per test is specified by the standard in use. Typically, standards call for 100 loading cycles per series, and between 16 and 30 total series per test.

2.3.2.7 Determination of Resilient Modulus

As mentioned in section 2.3.2.7, resilient modulus varies with changes in deviator stress and confining pressure. Thus, resilient modulus tests are typically run at a variety of combinations of deviator stresses and confining pressures. For a long time, the selection of an appropriate resilient modulus protocol for base, subbase, and subgrade materials was complicated by various test and analysis issues (Andrei et al., 2004). The NCHRP initiated Project 1-28A to synthesize a singular resilient modulus test method that harmonized the best features of four state-of-the-art test programs already in use. The protocols used in the development of Project 1-28A were: AASHTO T 292-91, AASHTO T 294-92, AASHTO T P46-94, and the NCHRP 1-28 Draft 96. The resulting test program provided researchers and pavement designers with a set of recommendations for resilient modulus characterization of base, subbase, and subgrade materials.

As noted previously, resilient modulus tends to increase with increasing confining pressure. This behavior has been recognized in pavement engineering, and

is commonly represented by a mathematical model based on experimental data. Prior to the publication of NCHRP Project 1-28A, a simplified power model of resilient modulus was most common. This model was first proposed by Moosazedh and Witczak in 1981 and is defined mathematically as

$$M_R = k_1 \theta^{k_2} \tag{2.2}$$

where M_R is resilient modulus, θ is bulk stress, and k_1 and k_2 are empirically derived constants. The constants k_1 and k_2 are unique to a given material and are independent of one another. Bulk stress is another means of quantifying confining pressure and deviator stress in a single term. In a pavement system, the bulk stress acting on a soil element is the combined pressure of the overlying pavement layers and the vertical wheel loads acting on the pavement. Bulk stress (θ) is defined as

$$\theta = \sigma_1 + \sigma_2 + \sigma_3 \tag{2.2}$$

where σ_1, σ_2, and σ_3 are the principal stresses acting on the specimen.

Research conducted in the years after Moosazeh and Witczak introduced their power model showed that most soils also exhibit decreasing stiffness with increasing shear (Andrei et al., 2004). The effect of shear stress on resilient modulus was not accounted for in Moosazedh and Witczak's power model. The NCHRP revised its resilient modulus protocol to account for these findings and introduced the harmonized NCHRP 1-28A power model in 2004. The NCHRP 1-28A power model for resilient modulus is defined as

$$M_R = k_1 p_a \left(\frac{\theta - 3k_6}{p_a}\right)^{k_2} \left(\left(\frac{\tau_{oct}}{p_a}\right) + k_7\right)^{k_3} \tag{2.3}$$

where M_r is resilient modulus, k_1, k_2, k_3, k_6, and k_7 are empirical constants, p_a is the atmospheric pressure, τ_{oct} is the octahedral shear stress, and θ is the bulk stress. As in

Moosazedh and Witczak's power model, the constants k_1, k_2, k_3, k_6, and k_7 are empirically derived, independent parameters unique to the material in question. The NCHRP 1-28A model effectively combines the influence of bulk stress and shear stress into a single equation.

Octahedral shear stress is defined as

$$\tau_{oct} = \frac{1}{3}\sqrt{((\sigma_1 - \sigma_2)^2 + (\sigma_1 - \sigma_3)^2 + (\sigma_2 - \sigma_3)^2)^2} \quad (2.4)$$

where τ_{oct} is octahedral shear stress, and σ_1, σ_2, and σ_3 are the principal stresses acting on the specimen. As reported previously, σ_1 is equal to the applied cyclic deviator stress plus the confining pressure, and σ_2, and σ_3 are equal to the confining pressure.

SECTION THREE

MATERIALS

3.1 RECLAIMED ASPHALT SHINGLES

Asphalt roofing shingles consist of a thin cellulose or fiberglass foundation saturated with asphalt (19 to 36% by weight). The cellulose i.e. organic felt backing was used exclusively for many years until concerns over asbestos prompted the development of fiberglass backings. Ceramic-coated natural sand-size rock (20 to 38% by weight) and a mineral filler/stabilizer (8 to 40% by weight consisting of limestone, silica, dolomite, etc.) are added to the asphalt layer (Shingle Recycling Organization, 2005). Ninety percent of the mineral filler is smaller than 0.15-mm, and 70 % is smaller than 0.08 mm.

Waste shingles are classified either as manufacture scrap or tear-offs from demolitions or re-roofing projects. Roofing shingles are typically replaced every 10 to 30 years. Thus, the shingles taken from a housing demolition or re-roofing job can be anywhere from ten to thirty years in age, or older depending on the situation. As a result, most “tear-offs” are derived from shingles constructed with a cellulose felt backing. However, as more and more roofs are constructed with fiberglass materials, the presence of the cellulose backing in “tear-offs” will diminish. Scrap shingles taken from fabricated housing plants, construction companies, and shingle manufacturers are generally less than one year in age, and composed primarily of shingles constructed with a fiberglass backing (Crivit, 2005). Hooper and Marr (2004) suggested that tear-off derived RAS should exhibit similar performance to manufacturer scrap derived RAS provided all wood, nails, plastic and other residue materials are removed.

Shingles selected for recycling must be free of asbestos (WDNR limits to 1%), wood, nails, plastic, styrofoam and other excess materials. These materials are removed by hand and discarded. The shingles are then ground, screened and graded to produce RAS. Recycling facilities utilize varying combinations of these steps to produce different gradations of RAS. RAS gradations typically are classified according to the maximum particle size present in the mix. Thus, a 19-mm minus RAS gradation contains particles 19-mm in diameter and smaller.

RAS samples utilized in this study were obtained from the Stratford Building Supply Co. (Stratford, WI) and the Bruce Landscaping Co. (Verona, WI). The Stratford Building Supply grinds waste shingles once over and then screens at three size intervals: 51-mm minus, 25-mm minus, and 19-mm minus. The Bruce Landscaping Co. uses a slightly different procedure. The waste shingles are ground once and then screened at 51-mm minus. They are then re-ground. Afterwards, the shingles are graded a second time using a finer screen to produce a final gradation of 10-mm minus. A 5-mm minus gradation was obtained by screening the 25-mm minus gradation through a 5-mm sieve. A photograph (not to scale) of the maximum particle size for each RAS gradation is shown in Figure 3.1.

The RAS obtained from the Stratford Building Supply Co. included tear-offs from construction jobs undertaken by the company, and manufacturer scrap from the nearby Wausau Housing Co. Based on visual inspection, the Stratford Building Supply Co. mixes contained mostly manufacturer scrap shingles, however; the exact ratio of tear-off to scrap material was unknown. The RAS obtained from the Bruce Co. included tear-offs from demolition and construction jobs undertaken by the company, as well as manufacturer scrap obtained from housing fabricators in the Madison area. Based on visual inspection, the Bruce Co. mix contained mostly tear-offs, however; the exact ratio of tear-off to scrap material was unknown.

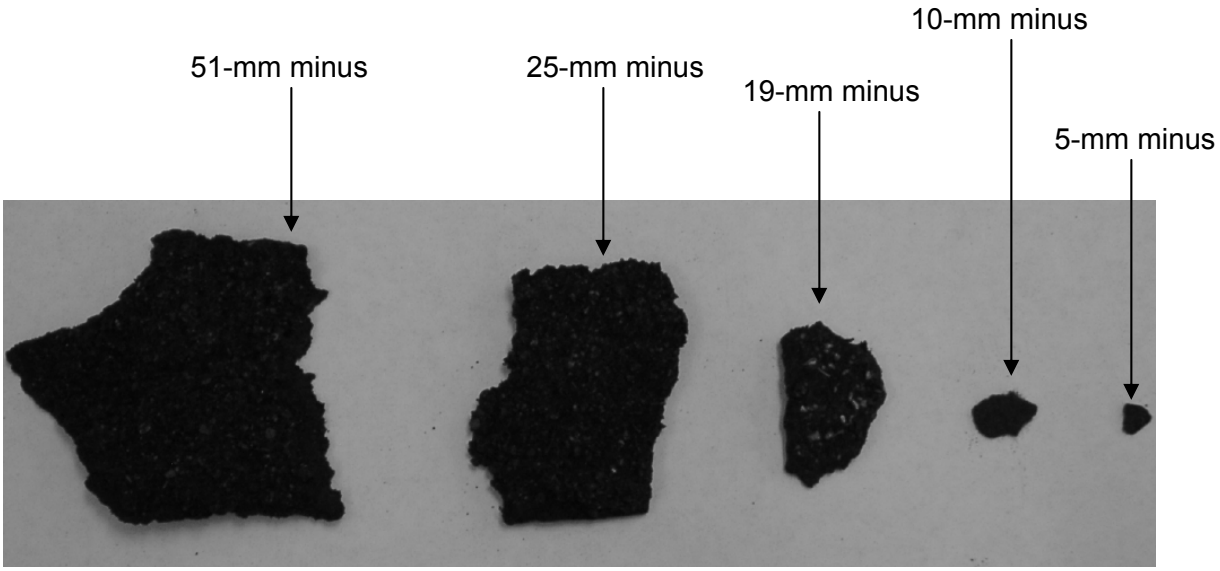

Figure 3.1 Maximum particle sizes for 5 RAS gradations

3.2 SELECTION OF SOILS FOR COMPOSITE MIXTURES

The objective of this study was to qualify the functionality of RAS as an additive to or replacement for soils and aggregates typically used in aggregate base course (AB), subbase course (ASB), and working platform or embankment fill applications. Wisconsin Department of Transportation (WisDOT) Grade 2 granular backfill and Boardman silt were chosen as representative aggregate and soil. The index properties of these materials are summarized in Table 3.1. The compaction characteristics of each material were determined using ASTM D 698 (Standard Proctor compaction test). Optimum water content and maximum dry density are listed in Table 3.2. The grain size curves of Grade 2 granular backfill and Boardman silt were determined using ASTM D 422. The grain size curves are included in Appendix A.

WisDOT Grade 2 granular backfill is a manufactured aggregate quarried from limestone and dolomite formations near Madison, WI. The Grade 2 Granular Backfill used in this study was collected from a section of Wisconsin State Highway (STH) 60 under re-construction. Grade 2 granular backfill classifies as poorly graded gravel with some silt and sand (GP-GM) by the Unified Soil Classification System (USCS), and is recognized as a medium-sized aggregate by WisDOT specifications. Grade 2 granular backfill is most commonly used as base course in road construction. Per WisDOT specifications, Grade 2 granular backfill must occupy at least the top 25 cm of base course in pavement structures.

Boardman silt is a naturally occurring soil from the Columbia River region near Boardman, OR. Boardman silt is classified as sandy silt with a liquid limit of 22, plasticity index of 1 and a specific gravity of solids of 2.73. The fines content is 76% and the sand content is 24%. Boardman silt was chosen for this study because it represents a possible fill material and was readily available for use at the University of Wisconsin-Madison Geotechnical Laboratory.

Table 3.1 Index properties

Soil Type	USCS Classification	Liquid Limit	Plastic Limit	Plasticity Index	% Gravel	% Sand	% Fines
WisDOT Grade 2 Granular Backfill	GP-GM	-	-	-	70	22	8
Boardman Silt	ML	22	21	1	0	24	76

Table 3.2 Compaction characteristics

Soil Type	Compactive Effort	Optimum Water Content (%)	Max. Dry Unit Weight (kN/m^3)
WisDOT Grade 2 Granular Backfill	Standard	10	21.0
Boardman Silt	Standard	15	16.5

3.3 COLUMBIA FLY ASH

Fly ash is a byproduct released during coal combustion. Fly ash is composed of the inorganic, incombustible material present in coal. This material is fused into a glassy, amorphous structure during combustion and is suspended in the exhaust gases. Fly ash solidifies out of the exhaust and is collected by electrostatic precipitors or filter bags. Because the material solidifies while suspended in gas, fly ash particles are generally spherical in shape and range in size from 0.5 μm to 100 μm. Fly ash can react with water, calcium hydroxide, and alkali to form cementitious compounds and is often used as a high-performance filler in many concrete mixes. In recent years, fly ash has also been used as a stabilizing additive to road bases, structural fills, embankments, and soil foundations.

Fly ashes are classified as class C, class F, or non-specification according to the presence or absence of several different compounds as specified in ASTM C 618. A class C fly ash from the Columbia Power Plant near Portage, WI was chosen for this study. The compositional properties of Columbia fly ash, Class C fly ash, and Class F fly ash are summarized in Table 3.3 (Edil et al., 2006).

Table 3.3 Compositional properties of Columbia, Class C, and Class F fly ashes (after Edil et al., 2006)

Fly Ash	**Strength Activity @ 7 Days, min (%)**	**LOI (%)**	**CaO (%)**	**SiO_2 (%)**	**Al_2O_3 (%)**	**Fe_2O_3 (%)**
Columbia	87	0.7	22.3	31.1	18.3	6.1
Class C	75	6.00 Max.	-	SiO_2+Al_2O_3+Fe_2O_3 50.0 min.		
Class F	75	6.00 Max.	-	SiO_2+Al_2O_3+Fe_2O_3 70.0 min.		

Note: LOI = loss on ignition.

SECTION FOUR

LABORATORY PROCEDURES

4.1 SAMPLE DESIGNATION

RAS samples were designated according to the maximum RAS particle size, and ratio of RAS to Grade 2 granular backfill or Boardman silt. Maximum RAS particle size was denoted using the letters A through E. The maximum RAS particle size indicator is the first character listed in the sample ID. The corresponding particle sizes for each letter are shown in Table 4.1. The maximum particle sizes ranged from 51-mm to 5-mm.

The sample composition indicator is the second character listed in the sample ID. Samples made entirely of RAS were indicated by the number 1. The number 2 indicated an RAS sample blended with either Grade 2 granular backfill or Boardman silt. Mixtures of RAS and Grade 2 granular backfill or silt were blended at a 50:50 ratio by mass.

Pure samples of Grade 2 granular backfill and Boardman silt were tested to provide a performance comparison between RAS and typical field materials. In these situations, the pure Grade 2 granular backfill and Boardman silt samples were identified according to the RAS gradation with which they were being compared. Pure Grade 2 granular backfill and Boardman silt samples were indicated by the number 3. Additionally, the composition indicator was accompanied with a subscript denoting the added material. A subscript G indicated Grade 2 granular backfill, and a subscript S indicated Boardman silt. A subscript N indicated a pure RAS sample devoid of Grade 2 granular backfill or Boardman silt. Sample composition indicators are listed in Table 4.2.

Example sample designations include: $A1_N$, $E2_S$, or $B3_G$. The first one indicates a sample composed of entirely of RAS with a maximum particle size of 51-mm. The second one indicates a sample composed of RAS and Boardman silt. The RAS and Boardman silt are blended at a 50:50 ratio by mass, and the maximum particle size of the RAS is 5-mm. The third one indicates a sample composed entirely of Grade 2 granular backfill. For the purposes of analysis, the Grade 2 granular backfill is being compared to RAS having a maximum particle size of 25-mm Table 4.3 is a summary of all sample IDs used for this study.

Table 4.1 Maximum RAS particle size indicators

Group Name	Maximum RAS Particle Size (mm)
A	51
B	25
C	19
D	10
E	5

Table 4.2 Numeric indicator of RAS to aggregate or soil ratio

Numeric Indicator	RAS Content (%): Grade 2 or Silt Content (%)
1	100:0
2	50:50
3	0:100

Table 4.3 Complete Sample Inventory

Sample ID	RAS Size (mm minus)	RAS Content (%)	Grade 2 Granular backfill Content (%)	Boardman Silt Content (%)
$A1_N$	51	100	0	0
$B1_N$	25	100	0	0
$B2_G$	25	50	50	0
$B3_G$	25	0	100	0
$C1_N$	19	100	0	0
$D1_N$	10	100	0	0
$E1_N$	5	100	0	0
$E2_S$	5	50	0	50
$E2_G$	5	0	0	100

4.2 PARTICLE SIZE ANALYSIS

A primary objective of the experimental program was to determine the relationship between the particle size characteristics and mechanical properties of RAS. The particle size distributions of RAS were determined according to ASTM D 422. Particle size analyses were also performed on Grade 2 granular backfill and Boardman silt. Particle size analyses were conducted using samples of at least 1000 g in accordance with ASTM specifications.

Samples were first wet-sieved through a No. 200 (0.075-mm opening) sieve to separate coarse and fine particles. The coarse portion of the Grade 2 granular backfill and Boardman silt was oven dried at 105^{o} C for 24 hours, and the fine particles were allowed to settle in the standing water left over from the wet-sieving process. The coarse RAS particles were air dried instead because the oven heat tended to bind the particles together. After drying, the coarse portions were dry-sieved and separated into constituent size fractions using ASTM specified sieves and a mechanical shaker. The particle size characteristics of the fine portions were measured using a hydrometer analysis. Images of the mechanical sieve shaker, sieves, and sieving materials are shown in Figure 4.1.

4.3 COMPACTION

Standard Proctor (ASTM D 698) compaction tests were used to determine the maximum dry unit weight and optimum water content of RAS, RAS-Grade 2 granular backfill, RAS-Boardman silt, and fly ash stabilized RAS (S-RAS). All materials were air dried prior to compaction. The materials were then spread on a large pan and hydrated with a spray bottle. Tap water was used to hydrate all samples. Composite and stabilized mixtures (RAS-Grade 2, RAS-Boardman silt, and S-RAS) were blended thoroughly prior to hydration. The samples were stirred thoroughly during hydration to

ensure uniform mixing. After mixing, samples were placed into large plastic bags and allowed to equilibrate for a set period of time prior to compaction. S-RAS specimens were allowed to equilibrate for approximately one hour. Samples devoid of fly ash were allowed to equilibrate for 16 to 24 hours as specified by ASTM standards.

Equilibrated samples were then placed loosely into the compaction mold and compacted with a manual rammer in a series of three lifts. The mold size and blow count were chosen according to the particle size characteristics. A 102 mm diameter mold was used if 20% or less by mass of the specimen material was retained on a No. 4 (4.75-mm opening) sieve. A 152 mm diameter mold was used if more than 20% by mass of the sample material was retained on a No. 4 sieve and less than 20% by mass of the sample material was retained on a 10-mm sieve. Compaction molds were 116 mm in height. The ASTM standard for standard Proctor compaction effort specified 25 blows per layer for specimens compacted in the 102 mm diameter mold, and 56 blows per layer for specimens compacted in the 152 mm diameter mold.

The mold, base plate, and compacted specimen were weighed after compaction. A portion of the sample totaling at least 500 g was used to determine water content. Samples selected for water content determination were weighed immediately after compaction and oven dried overnight at 105^{o}C. Samples were weighed again the next day to determine dry weight. Samples consisting solely of RAS (no additive material) were air-dried because the heat of the oven tended to meld the shingles to the pans they were drying in. The RAS water content samples were weighed repeatedly until a consistent dry weight was observed. Photographs of the compaction equipment are shown in Figure 4.2.

Figure 4.1 Photograph of (a) mechanical sieve shaker, and (b) dry sieves

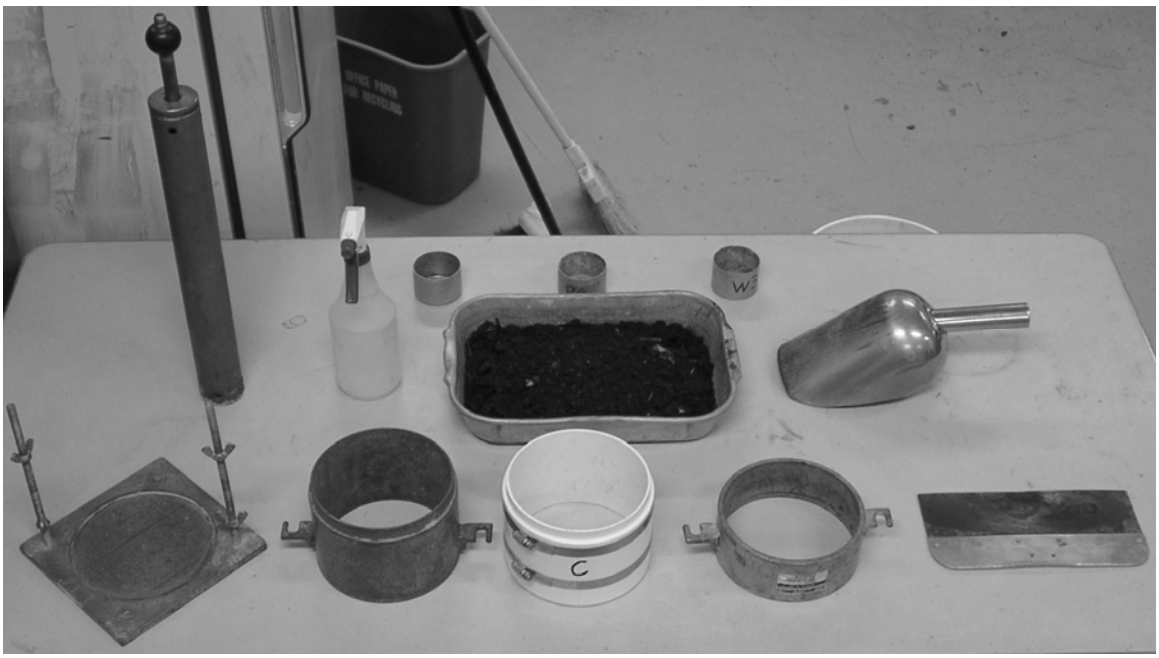

Figure 4.2 Photograph of compaction test equipment

4.4 CALIFORNIA BEARING RATIO

The California Bearing Ratio (CBR) (ASTM D 1883) test was used to determine the penetrative resistance of RAS, RAS-Grade 2 granular backfill, RAS-Boardman silt, and S-RAS mixtures. The ASTM standard mandated that CBR tests be run on material passing the 19-mm sieve. Material retained on the 19-mm sieve must be removed and replaced by an equal amount of material passing the 19-mm sieve and retained on the No. 4 sieve. This step was omitted for RAS specimens that contained particles larger than 19-mm. RAS specimens obtained from the Stratford Building Supply Co. and the Bruce Landscaping Co. were prepared to a specific grade at the respective recycling facilities. Removing particles greater than 19-mm would have altered the particle size characteristics of the field specimens. A primary objective of this study was to observe how RAS strength varied with gradation. Altering the facility-specified particle size characteristics of the RAS prior to CBR testing would have been detrimental to the research objectives. RAS specimens were tested "as is" and the outcomes of this procedural variation are accounted for in the results and analysis section.

Samples chosen for CBR testing were compacted in 152 mm diameter, 116 mm deep molds at a minimum of 95% of the standard Proctor maximum dry unit weight, and within $\pm$ 0.5% of the optimum water content in accordance with ASTM D 698. Samples containing fly ash were compacted in PVC molds (as opposed to metal compaction molds), sealed in plastic wrap, and cured in a 100% humidity room for a predetermined time period prior to CBR testing. Unstabilized samples were tested immediately after compaction. A portion of the excess test materials were taken after compaction to determine moisture content.

Compacted samples were then prepped for CBR testing. Two annular metal weights having a total mass of 4.54 kg were loaded on the exposed upper surface of the compacted sample. The annular weights have a center hole approximately 54 mm

in diameter through which a 50 mm diameter piston was slotted. The piston-weight assembly, compacted sample, mold, and baseplate were placed in a sturdy pan. Samples were not soaked prior to the CBR test.

The CBR sample was loaded into the compression machine and the penetration piston was seated using the smallest load possible. The piston was penetrated into the sample at a rate of 1.27 mm/min. Displacement and load readings were measured using TestWorks and a Windows PC. The piston was penetrated to a depth of 12.7 mm. After testing, the sample was removed from the testing apparatus and final moisture contents were measured. Photographs of the assembled CBR sample and test apparatus are shown in Figure 4.3.

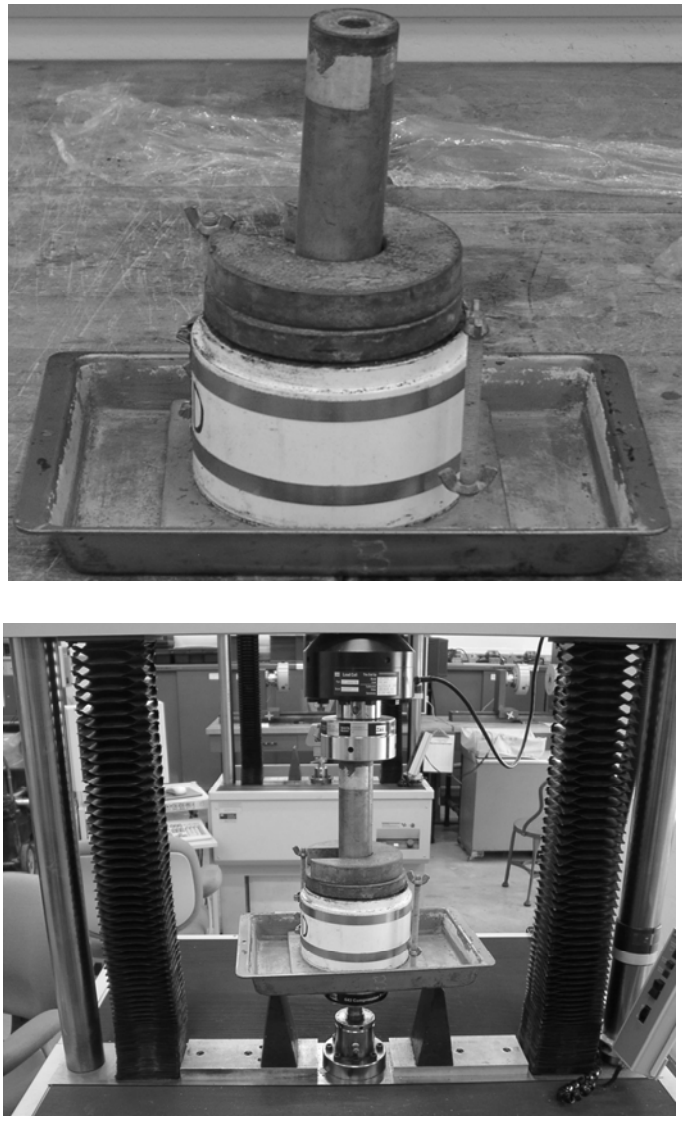

Figure 4.3 Photograph of (a) CBR sample and (b) CBR sample loaded into the compressive load frame

4.5 RESILIENT MODULUS

4.5.1 Laboratory Procedure

The resilient modulus (NCHRP 1-28 A) test was used to determine the stiffness of RAS, RAS-Grade 2, and S-RAS mixtures under stress conditions designed to simulate moving wheel loads over flexible pavement. RAS-Boardman silt mixes were not tested for resilient modulus.

Samples chosen for resilient modulus testing were compacted at 95% of the maximum dry unit weight, and within $\pm$ 0.5% of the optimum water content. Specimens were compacted in a 102 mm diameter, 203 mm deep mold. The NCHRP 1-28 A protocol required that particles larger than 25-mm be scalped off prior to testing, however; this procedure was omitted for the same reasons as those listed in the CBR laboratory procedure section. S-RAS samples were compacted in a PVC mold, sealed with shrink wrap, and cured in a 100% humidity room for a predetermined time period prior to resilient modulus testing. Samples devoid of fly ash were compacted in a split metal mold and tested immediately after compaction. Representative samples of excess test material were taken after compaction to determine moisture content.

A pressurized sample extruder was used to remove cured S-RAS samples from the PVC molds. Unstabilized samples were removed by hand from the split metal mold. The specimen initial length and diameter were measured prior to resilient modulus testing. Test specimens were then fitted with an upper end platen and placed on the base pedestal of the triaxial cell. Geotextiles were placed between the specimen and the end contacts. A latex membrane was fitted over the sample and end platens. After fitting, the latex membrane was secured to the end platens with O-rings. The specimen was then sealed inside the triaxial chamber. The loading piston was lowered through a circular opening in the triaxial cover plate and slotted into the loading joint at the top of

the end platen. The loading piston was oiled with WD-40 prior to insertion into the cell to maintain a frictionless interface between the loading piston and cell cover. The outer contact points between the piston and cell cover were filled with vacuum grease to prevent cell pressure leakage during the test. The triaxial cover plate was sealed tightly.

The triaxial cell and loading piston were then positioned inside the loading frame. The piston was coupled to the arm of the loading frame using a smooth ball bearing. The loading arm was lowered onto the ball bearing using a high hydraulic pressure pump, and seated using a load of less than 0.02 kN. The confining air pressure supply line was then connected to the triaxial chamber, and confining air pressure (as specified by the NCHRP 1-28 A protocol) was applied to the specimen. An initial contact stress equal to 20% of the confining pressure was applied to the specimen to ensure that the load piston remained in contact with the end platen during testing. External LVDTs were used to measure axial deformation. The LVDTs were placed on top of the triaxial cell cover and adjusted as needed. A photograph of the sample, load piston, and triaxial cell chamber is shown in Figure 4.4.

The load cycles were controlled and monitored via a LabView testing template specifically adapted for the NCHRP protocol by Professor Peter Bosscher of the University of Wisconsin-Madison. The LabView testing template was run on a Windows compatible PC. The LabView template recorded confining pressure and loading stress for each loading cycle, and deformation measurements from both LVDTs. The resilient modulus test was initiated after a final instrument check.

Specimens were tested for resilient modulus using the NCHRP 1-28 A protocol for cohesive subgrades. Confining pressure, contact stress, cyclic stress and maximum stress for each loading sequence of the cohesive protocol are shown in Table 4.4.

First, the triaxial specimen was conditioned with a series of 1000 load pulses. A full load pulse consisted of a 0.2 second period of loading, followed by a 0.8 second rest

period prior to the next load pulse. An individual load pulse in the conditioning phase was equivalent to a maximum axial stress of 53.8 kPa and cyclic stress of 48.3 kPa.

After the conditioning phase was completed, the specimen was tested using the sequence of loading repetitions outlined in the NCHRP 1-28 A cohesive protocol. The number of loading repetitions used for a sequence is 100, save for the initial conditioning phase.

Once the loading sequences were completed, the cell pressure was reduced to zero, and the sample was removed from the triaxial cell. The latex membrane was removed and final measurements of sample length and diameter were recorded. S-RAS specimens were then tested for unconfined compressive strength, whereas; unstabilized RAS specimens were disposed.

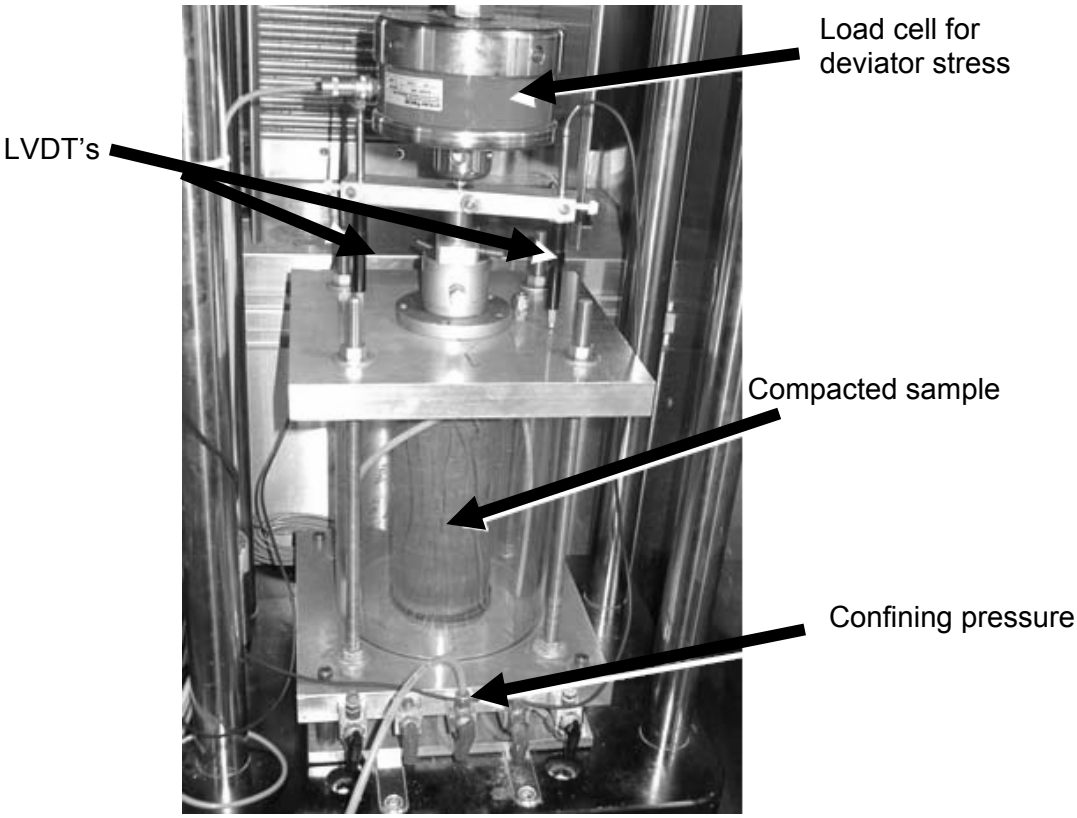

Figure 4.4 Photograph of compacted specimen loaded in resilient modulus cell

Table 4.4 NCHRP 1-28 A protocol for resilient modulus of cohesive subgrades

Sequence	Confining Pressure (kPa)	Contact Stress (kPa)	Axial Stress (kPa)	Deviator Stress (kPa)	Number of Repetitions
0	27.6	5.5	48.3	53.8	1000
1	55.2	11	27.6	38.6	100
2	41.4	8.3	27.6	35.9	100
3	27.6	5.5	27.6	33.1	100
4	13.8	2.8	27.6	30.4	100
5	55.2	11	48.3	59.3	100
6	41.4	8.3	48.3	56.6	100
7	27.6	5.5	48.3	53.8	100
8	13.8	2.8	48.3	51.1	100
9	55.2	11	69	80	100
10	41.4	8.3	69	77.3	100
11	27.6	5.5	69	74.5	100
12	13.8	2.8	69	71.8	100
13	55.2	11	96.6	107.6	100
14	41.4	8.3	96.6	104.9	100
15	27.6	5.5	96.6	102.1	100
16	13.8	2.8	96.6	99.4	100

4.5.2 Data Analysis

Output data from the resilient modulus test were recorded into a text file. Data recorded in the text file included high and low deformation measurements for each LVDT, cell pressure readings for each load cycle, and the high and low deviator stresses for each loading event. The data in the text files were loaded into an automated Excel spreadsheet and analyzed according to the NCHRP procedure.

In accordance with the NCHRP 1-28 A protocol, resilient modulus was calculated using dynamic deviator stress.

$$\sigma_D = \sigma_{d,h} - \sigma_{d,l} \tag{4.1}$$

where σ_D is the dynamic deviator stress, $\sigma_{d,h}$ is the highest recorded deviator stress, $\sigma_{d,l}$ is the lowest recorded deviator stress. The lowest deviator stress is the stress imposed on the sample during rest periods i.e. stress imposed by the weight of the loading platen and the seating load. The maximum deviator stress is the stress imposed during a loading event i.e. stress imposed by the weight of the loading platen, seating load, and the NCHRP specified load. The Excel spreadsheet automatically calculated dynamic deviator stress for every loading event in the sequence. Additionally, the Excel spreadsheet calculated bulk stress and octahedral shear stress for each loading event in the sequence (Eqs. 2.2 and 2.4).

The deformation readings obtained from the LVDTs were used to calculate resilient deformation. Resilient deformation was calculated as

$$\Delta_R = \Delta_{r,H} - \Delta_{r,U} \tag{4.4}$$

where Δ_R is the resilient deformation for a given load, $\Delta_{r,H}$ is the LVDT measurement during loading, and $\Delta_{r,U}$ is the LVDT measurement during the rest period between loading events. Resilient deformation was calculated for both LVDTs and averaged.

Resilient strain was calculated as

$$\varepsilon_R = \frac{\Delta_R}{h_{ave}} \tag{4.5}$$

where ε_R is resilient strain, Δ_R is the resilient deformation, and h_{ave} is the average height of the test specimen. Average height is the average of the specimen heights measured prior to and after testing. Resilient strain was calculated for both LVDTs and averaged.

Resilient modulus was calculated using average resilient strain. Resilient modulus was calculated automatically by Excel for each loading event in the NCHRP sequence (Eq. 2.1).

4.5.3 Modeling Techniques

Resilient modulus was calculated for each loading event in the NCHRP 1-28 A sequence. An average resilient modulus for each sequence of loading events was calculated and used to formulate the parameters for the NCHRP 1-28 A power model (Eq. 2.3). The NCHRP defines resilient modulus for a sequence of loading cycles as the average of the resilient moduli for the last five cycles of that sequence. The average resilient moduli from each loading sequence for a single specimen were fitted to the NCHRP 1-28 A power model using the SOLVER application of Microsoft Excel. The resulting k-parameters were recorded and used to determine a predicted resilient modulus for a given material under a specified stress state.

4.6 UNCONFINED COMPRESSION

The unconfined compression test (ASTM D 2166) was used to determine the axial strength of S-RAS. Unconfined compression tests were run on samples that had completed resilient modulus testing. Resilient modulus testing did not result in failure of the test specimen, therefore; the specimen could be reused to minimize the need for additional samples.

Specimens were loaded into the loading cell and compressed at a rate of 0.21% strain per minute. For a 203 mm long sample, this equated to a compression rate of approximately 0.43 mm per minute. Displacement and load readings were measured using TestWorks and a Windows PC. The sample was compressed to failure i.e. peak compressive strength. Portions of the sample were taken for moisture content measurements after unconfined compression testing was completed. The moisture contents were used as a reference, but were not, however; used to calculate dry unit weight.

SECTION FIVE

RESULTS AND ANALYSIS

5.1 PROPERTIES OF RAS, RAS-GRADE 2 GRANULAR BACKFILL, AND RAS-BOARDMAN SILT MIXTURES

5.1.1 Particle Size Analysis Results

The gradation characteristics of each RAS sample were analyzed according to ASTM D 422. As was mentioned previously, RAS samples were obtained from either the Stratford Building Supply Co. or the Bruce Landscaping Co. The Stratford Building Supply Co. provided three different gradations: a 51-mm minus gradation ($A1_N$), a 25-mm minus gradation ($B1_N$), and a 19-mm minus gradation ($C1_N$). A 5-mm minus gradation ($E1_N$) was developed by sieving $A1_N$ through a 5-mm mesh sieve. The Bruce Landscaping Co. provided a single gradation of 10-mm minus ($D1_N$). The Stratford shingle samples were sieved only once after being ground, and based on visual inspection, contained mostly manufacturer scrap shingles. The Bruce Co. sample was ground, sieved through a 51-mm mesh sieve, then re-ground and re-sieved through a 10-mm mesh sieve. Based on visual inspection, the Bruce Co. contained mostly tear-offs. The particle size curves for each RAS sample are shown in Figure 5.1. The important particle size parameters and USCS classifications of each RAS specimen are shown in Table 5.1.

Each specimen was classified according to the USCS system, however; these classifications are idealized in every sense. The USCS system idealizes soil particles as spheres and classifies them according to diameter. RAS particles are not spherical in nature. Instead, they are flat and plate-like. The majority of RAS particles are significantly longer than they are thick i.e. length to thickness aspect ratios of 25 to 50.

As the RAS particles become smaller, this aspect ratio decreases. Additionally, RAS particles become more equidimensional when ground to sizes smaller than 1 mm. At this point, the shingle has been separated mostly into its constituent parts. These constituents i.e. sand and mineral particles, asphalt globules, etc., are more equidimensional in nature. The organic or fiberglass foundation is the constituent material contributing most significantly to the plate-like nature of larger RAS particles.

In light of these characteristics, the USCS system is not wholly sufficient in classifying RAS gradations. However, at this time, a better means of classifying RAS mixes does not exist. The development of a specialized RAS particle classification system would benefit future study. Parameters of interest might include length to thickness aspect ratio, maximum particle size, percentage of plate-like particles, etc. Additionally, the RAS gradations could be characterized according to the relative percentages of tear-off and scrap material present in the mix and asphalt content.

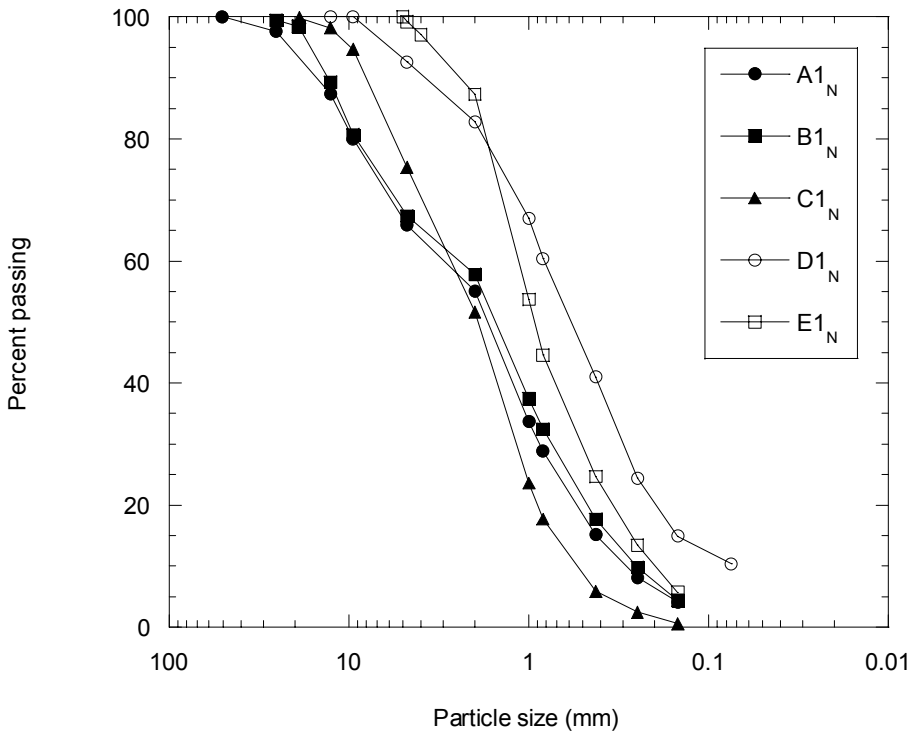

Figure 5.1 Particle size curves for 5 RAS gradations

Table 5.1 Particle size parameters and USCS classification of 5 RAS gradations

Sample Name	Maximum Particle size (mm)	D_{60} (mm)	D_{30} (mm)	D_{10} (mm)	C_u[1]	C_z[2]	Gravel[3] Fraction (%)	Sand[4] Fraction (%)	Fine[5] Fraction (%)	USCS Classification
$A1_N$	51	2.9	0.9	0.3	10	1	35	64	1	SW
$B1_N$	25	2.5	0.8	0.3	8	1	33	65	2	SW
$C1_N$	19	2.7	1.2	0.5	5	1	25	74	1	SP
$D1_N$	10	0.8	0.3	0.08	10	1	8	81	11	SW-SM
$E1_N$	5	1.1	0.5	0.2	6	1	<1	96	3	SW

[1]C_u = Coefficient of Uniformity = D_{60} / D_{10} where D_x is the particle size corresponding to x% passing
[2]C_z = Coefficient of Curvature = D_{30}^2 / (D_{60} * D_{10})
[3]Retained on No. 4 sieve with mesh opening of 4.75-mm
[4]Passing No. 4 sieve but retained on No. 200 sieve
[5]Passing No. 200 sieve with mesh opening of 0.075-mm

As expected, $A1_N$ and $B1_N$ have the highest percentage of coarse particles. There is little difference between the gradation curves for these samples, save for the larger maximum particle size for $A1_N$. Both samples are made up of approximately 35% coarse particles. Both $A1_N$ and $B1_N$ classify as well-graded sand with gravel according to USCS specifications.

Sample $C1_N$ is more uniform than $A1_N$ and $B1_N$. Sample $C1_N$ contained a significant amount of wood. Bernie Wenzel, the recycling director the Stratford facility, indicated that $C1_N$ was prepared immediately after a large amount of wood scrap was run through the sieving chamber. As such, the residue wood may have altered the characteristic uniformity of $C1_N$. $C1_N$ classifies as poorly-graded sand with gravel by the USCS classification system.

The $D1_N$ specimen obtained from the Bruce Landscaping Co. has the highest percentage of fine particles of any RAS specimen tested. The $D1_N$ is also the only specimen containing more than 10% fines by mass. The increased percentage of fines is likely attributed to the second phase of grinding and sieving utilized by the Bruce Landscaping Co. in preparing the RAS. $D1_N$ classifies as well-graded sand with silt sized particles.

$E1_N$ consists of shingles graded from sample $B1_N$ using a 5-mm mesh sieve. $E1_N$ classifies as well-graded sand according to the USCS system. $E1_N$ contains 3% fines and has a D_{10} particle size of 0.2 mm.

The particle size characteristics of $A1_N$, $B1_N$, $C1_N$, and $E1_N$ were reevaluated after compaction to determine if the compactive energy resulted in any breakage of RAS particles and thereby altered the particle size characteristics. The particle size curves from this analysis are included in Appendix B. The act of compaction appeared to have little to no effect on the particle size characteristics of each specimen.

5.1.2 Compaction Test Results

The compaction characteristics of RAS were measured using ASTM D 698 (standard Proctor effort). Compaction curves for five RAS gradations are shown in Figure 5.2. The maximum dry unit weight and optimum water content for each specimen are summarized Table 5.2. The maximum dry unit weight of RAS ranged from 8.8 kN/m^3 (for $C1_N$ 19-mm minus) to 12.5 kN/m^3 (for $D1_N$ 10-mm minus). The optimum water contents ranged between 7% and 10% for all RAS gradations except for $D1_N$ which had an optimum water content of approximately 14.5%.

In general, RAS maximum dry unit weight decreases with increasing maximum particle size. While this is true for the Stratford samples, the Bruce Co. sample with a maximum particle size of 10 mm deviates from this trend. This implies that not only the size but the nature of the shingles is also important. Samples $A1_N$, $B1_N$, and $C1_N$ correspond to the three largest RAS sizes, however; they exhibited the lowest maximum dry unit weights of the five samples tested. Conversely, samples $D1_N$ and $E1_N$ are composed entirely of particles less than 10-mm, yet they exhibited maximum dry unit weights 2 to 4 kN/m^3 higher than samples $A1_N$, $B1_N$, and $C1_N$.

Compaction is a function of soil gradation (Holtz and Kovacs, 1981). In most situations, maximum dry unit weight increases with decreasing particle size uniformity. The differences in uniformity (C_u) between the 5 RAS gradations were minimal. Therefore, the differences in compactive behavior between the 5 RAS

Table 5.2 Standard Proctor compaction test results for 5 RAS gradations

Sample ID	RAS gradation (mm minus)	Optimum water content (%)	Maximum dry unit weight (kN/m^3)
$A1_N$	51	7.4	10.4
$B1_N$	25	9.8	9.9
$C1_N$	19	6.9	8.8
$D1_N$	10	14.2	12.5
$E1_N$	5	8	12.3

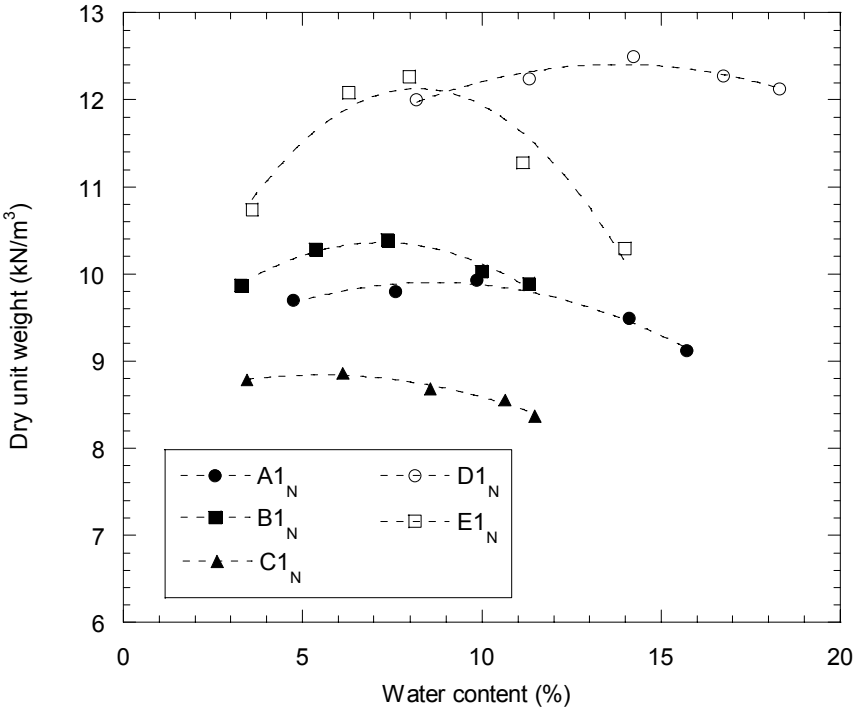

Figure 5.2 Standard Proctor compaction curves for 5 RAS gradations

gradations cannot be directly attributed to differences in particle size uniformity.

Compaction is also related to angularity and surface roughness as these factors would reduce the ease of packing. RAS particles larger than 10-mm are plate-like, angular around the edges, and covered with rough, sand-blasted surfaces. RAS particles smaller than 10-mm minus have smoother edges, weathered surfaces, and are generally less angular in shape. Additionally, more of the constituent particles i.e. sand and mineral filler, asphalt globules, etc., have been shaved off the surfaces and are capable of filling void spaces in RAS gradations of 10 mm resulting in a better graded material.

As shown in Figure 5.2., RAS gradations with a maximum particle size of 10-mm or less compacted at higher dry unit weights than RAS gradations with maximum particle sizes larger than 10-mm. Although RAS compactive behavior may be partially related to the minor variations in particle size uniformity between samples, the likelihood exists that variations in particle shape have a greater effect on compacted dry unit weight of RAS. In other words, RAS particles smaller than 10-mm are capable of packing more densely than RAS particles larger than 10-mm because RAS particles less than 10-mm are more equidimensional. Photographs of representative RAS particles smaller than 10-mm, and RAS particles larger than 10-mm are shown in Figure 5.3. Based on visual inspection under microscope, RAS becomes more equidimensional and its surface roughness decreases with decreasing particle size. This is observed most in RAS fines (passing No. 200 sieve). Therefore, RAS packing behavior improves with decreasing particle size.

Particle size of RAS is directly related to the process by which the RAS is produced. As mentioned previously, $A1_N$, $B1_N$, and $C1_N$ were obtained directly from the

Stratford Building Supply Co., whereas $D1_N$ was obtained from the Bruce Landscaping Co. ($E1_N$ was obtained by re-grading $A1_N$ down to 5-mm minus.) The Stratford Building Supply Co. and the Bruce Landscaping Co. utilize different techniques for processing and producing RAS. The Stratford Building Supply Co. uses a single cycle of sieving and grinding. The waste shingles are brought to the facility, screened for wood, metal and plastic, and then ground into a smaller, more manageable size. The ground shingles are then loaded in a cylindrical canister. A large circular sieve (25-mm opening) is fitted inside the canister and the shingles are spun inside until they have been broken down enough to pass through the sieve and onto the conveyor. The Bruce Landscaping Co. utilizes an additional phase of sieving and grinding in their RAS production process. Upon arrival at the facility, the waste shingles are ground and passed through the first sieving apparatus (51-mm opening). They are then re-ground, and re-graded using a finer sieve (10-mm opening). The second phase of sieving and grinding reduces the maximum particle size and increases the fines content of the RAS.

Sample $B1_N$ was mixed with Grade 2 granular backfill at a 50:50 mass-to-mass ratio ($B2_G$) and compacted according to ASTM D 698. Sample $E1_N$ was mixed with Boardman silt at a 50:50 mass-to-mass ratio ($E2_S$) and compacted according to ASTM D 698. The compaction curves for $B2_G$ and $E2_S$ are shown in Figures 5.4 and 5.5, respectively. Standard Proctor compaction curves for $B1_N$ and Grade 2 granular backfill ($B3_G$) are also given for reference on Figure 5.4, and Standard Proctor compaction curves for $E1_N$ and Boardman silt ($E3_S$) for reference on Figure 5.5. The results of the standard Proctor compaction tests on RAS-Grade 2 granular backfill, and RAS-Boardman silt mixes are summarized in Table 5.3 and 5.4, respectively. As expected, dry unit weight of Grade 2 granular backfill and Boardman silt decreased with increasing RAS content.

Figure 5.3 Photograph of RAS particles greater than 10 mm in size (left) and less than 10 mm in size (right)

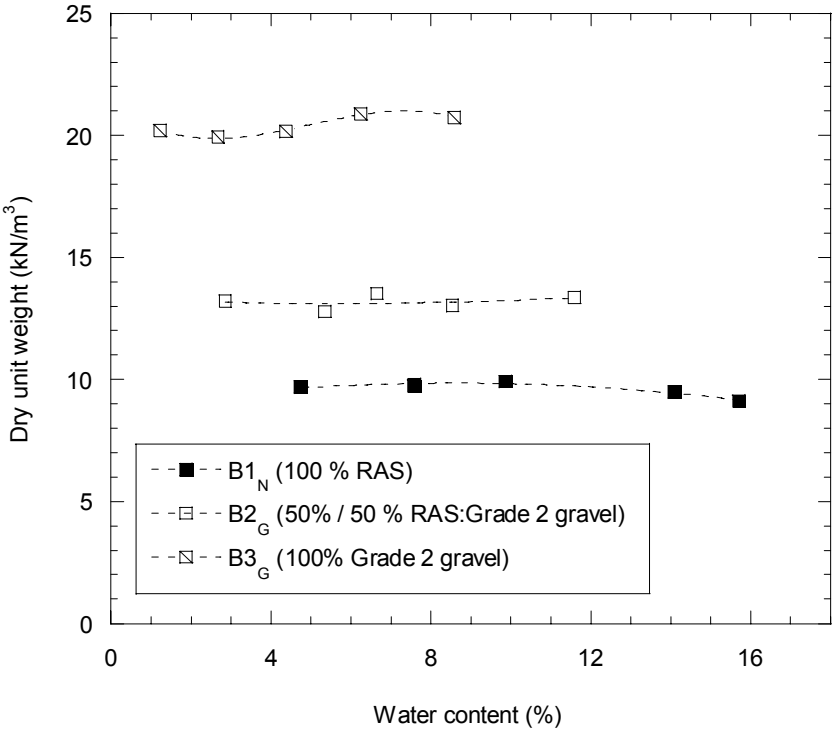

Figure 5.4 Standard Proctor compaction test – B series (25-mm minus)

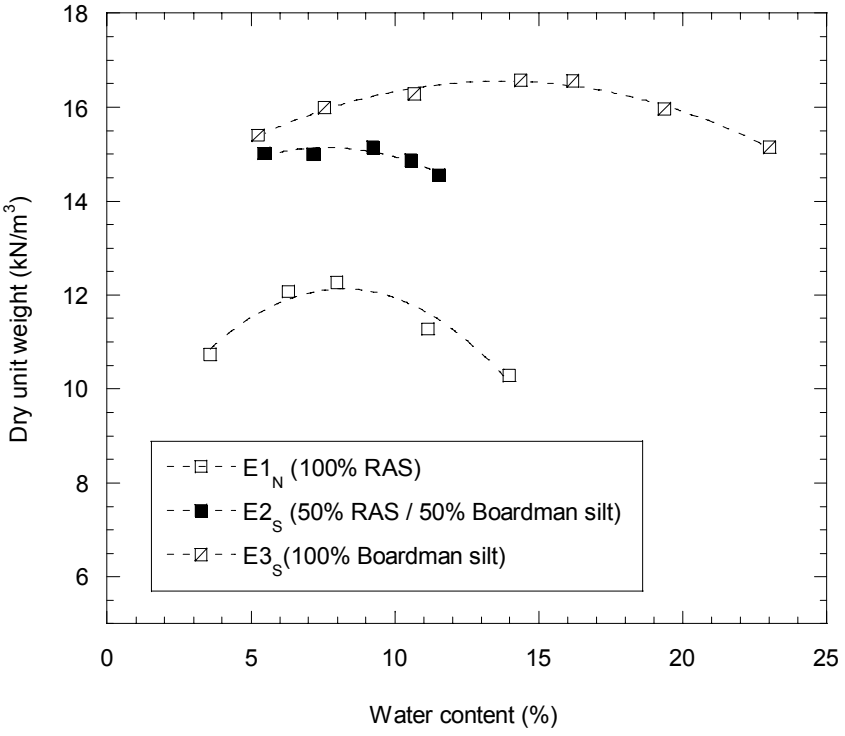

Figure 5.5 Standard Proctor compaction test – E series (5-mm minus)

Table 5.3 Standard Proctor compaction of RAS-Grade 2 mixtures

Sample ID	RAS Gradation (mm minus)	RAS Content (%)	WisDOT Grade 2 Content (%)	Optimum Water Content (%)	Maximum Dry Unit Weight (kN/m^3)
$B1_N$	25	100	0	9.8	9.9
$B2_G$	25	50	50	6.6	13.6
$B3_G$	25	0	100	6.2	21

Table 5.4 Standard Proctor compaction of RAS-Boardman silt mixes

Sample ID	RAS Gradation (mm minus)	RAS Content (%)	Boardman Silt Content (%)	Optimum Water Content (%)	Maximum Dry Unit Weight (kN/m^3)
$E1_N$	5	100	0	8	12.3
$E2_S$	5	50	50	9	15.2
$E3_S$	5	0	100	16	16.6

5.1.3 California Bearing Ratio Test Results

Penetrative resistance of RAS, compacted to 95% of standard maximum dry unit weight, was measured using California Bearing Ratio (CBR) tests (ASTM D 1888). Ninety-five percent relative compaction is a customary level of compaction specified for base course construction. The results of these tests are summarized in Table 5.5. Suggested CBR for soils used in pavement structures are shown in Table 5.6.

The CBR of RAS is comparable to that of a poor subgrade according to the guidelines outlined in Table 5.6. In summary, pure RAS is susceptible to penetration and possible particle crushing under locally intense pressures.

Sample $B1_N$ was mixed with WisDOT Grade 2 granular backfill at a 50:50 mass-to-mass ratio, compacted to 95% of standard maximum dry unit weight, and tested for CBR according to ASTM standards. Sample $E1_N$ was mixed with Boardman silt at a 50:50 mass-to-mass ratio, compacted to 95% of standard maximum dry unit weight, and tested for CBR according to ASTM standards. Pure samples of Grade 2 granular backfill and Boardman silt were also tested for CBR and used for reference. The results of these tests are summarized in Table 5.7. Plots of CBR versus RAS content for the RAS-Grade 2 mix and the RAS-Boardman silt mix are shown in Figure 5.6.

The RAS-Grade 2 mix and the RAS-Boardman silt mixes have slightly improved CBR compared to pure RAS. CBR of Grade 2 granular backfill and Boardman silt decreased dramatically with increasing RAS content. In summary, mixtures of RAS and either Grade 2 granular backfill or Boardman silt are decidedly more susceptible to penetrative deformation than pure Grade 2 or Boardman silt.

CBR is an index property indicative of resistance to local penetration and possible particle crushing under locally intense pressures. The test was designed to measure the rutting potential of compacted but unpaved roads. Although CBR is an

indicator of the localized material strength, it is by no means a comprehensive measure of total material stiffness. CBR is best utilized as a supplement to resilient modulus and other material index properties. The results of CBR testing for RAS, RAS-Grade 2 granular backfill, and RAS-Boardman silt mixtures imply that RAS is not suitable for use in subbase or base course applications. However; further testing of RAS for resilient modulus indicates that the CBR results are not an absolute indicator of RAS performance as a substitute for virgin aggregates in base and subbase course.

Table 5.5 CBR results for 5 RAS gradations

Sample ID	RAS Gradation (mm minus)	CBR
$A1_N$	51	2
$B1_N$	25	2
$C1_N$	19	1
$D1_N$	10	3
$E1_N$	5	3

Table 5.6 Suggested CBR for soils used in pavement structures (from Hooper and Marr, 2003)

Pavement Course	Material	CBR
Base course	Good quality crushed rock	>80
	Good quality gravel	50 to 80
Subbase course	Good quality soil	30 to 50
	Very good	20 to 30
Subgrade	Good to fair	10 to 20
	Questionable to fair	5 to 10
	Poor	<5

Table 5.7 CBR of RAS / Grade 2 and RAS / silt mixtures

Sample ID	RAS Gradation (mm minus)	RAS Content (%)	Grade 2 / Silt Content (%)	CBR
$B1_N$	25	100	0	2
$B2_G$	25	50	50	3
$B3_G$	25	0	100	58
$E1_N$	5	100	0	3
$E2_S$	5	50	50	8
$E3_S$	5	0	100	20

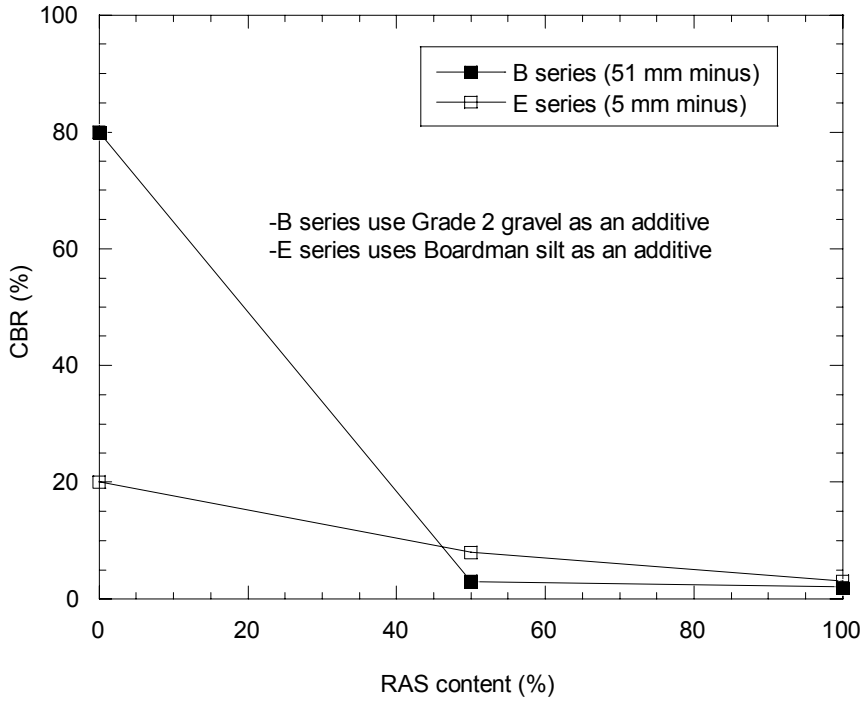

Figure 5.6 CBR of RAS-Grade 2 granular backfill and RAS-Boardman silt mixes

5.1.4 Resilient Modulus Test Results

Resilient modulus tests were conducted on RAS samples to determine the particle size characteristics, gradation, and compaction characteristics necessary to maximize resilient modulus. Particle size analyses, compaction tests, and CBR tests established a distinct hierarchy of performance among the 5 RAS gradations selected for the study. To prevent redundancy and to streamline the testing process, the RAS gradations with the poorest performance in the aforementioned testing sequence were not tested for resilient modulus. The RAS gradations chosen for resilient modulus testing were: 25-mm minus (B group), 10-mm minus (D group), and 5-mm minus (E group). The 51-mm minus RAS gradation (A group) and the 25-mm minus RAS gradation (B group) exhibited nearly identical particle size, compaction and CBR characteristics. Therefore, resilient modulus tests were run solely on the B group to minimize the need for additional samples. The 19-mm minus (C group) RAS gradation exhibited the lowest fines percentage, lowest maximum dry unit weight, and lowest CBR of the 5 RAS gradations. As such, the C group was not tested for resilient modulus.

The RAS gradations selected for resilient modulus testing were tested using the NCHRP 1-28 A protocol for cohesive subgrades. RAS was classified as a coarse, granular material, and had been proposed as supplement and/or replacement fill for base and subbase aggregates. According to NCHRP standards, RAS should then be tested using the 1-28 A protocol for base-subbase. However, the CBR test results showed that unstabilized RAS lacked the penetrative strength of sand or granular backfill. The performance of RAS in CBR testing was more akin to that of soft subgrade soil. The likelihood existed that the bulk stresses utilized in the NCHRP 1-28 A base-subbase protocol would strain unstabilized RAS specimens beyond the allowable limit. (The NCHRP 1-28 A procedure allowed no more than 5% strain during resilient

modulus testing.) A preliminary resilient modulus test was conducted on a 10-mm minus RAS specimen using the base-subbase protocol to determine if this was indeed correct. The 203 mm tall test specimen experienced 19-mm of permanent deformation over the duration of the test. The total deformation was equivalent to 9% strain, and was in excess of the limit allowed by the NCHRP. Therefore, unstabilized RAS was tested for resilient modulus using the cohesive protocol rather than the NCHRP base-subbase protocol because the bulk stresses used in the base-subbase protocol strained the preliminary RAS specimen beyond the limits allowed by the NCHRP. Furthermore, RAS specimens exhibited some apparent cohesion perhaps because of asphalt binding.

The cohesive protocol consisted of 16 load sequences (see Table 4.4). Each sequence featured a different combination of confining pressure and deviator stress. Resilient modulus varies with both confining pressure and deviator stress. Deviator stress is equivalent to axial stress plus contact stress and is used to calculate octahedral shear stress. The deviator stress loads deforms the specimen axially whereas confining pressure provides lateral support and restrains axial compression. Therefore, both the effect of confining pressure and octahedral shear stress must be accounted for when determining resilient modulus.

RAS resilient modulus data was analyzed first by holding confining pressure constant and evaluating the variation of resilient modulus with increasing octahedral shear stress. Afterwards, RAS resilient modulus data was reanalyzed by holding deviator stress constant and evaluating the variation of resilient modulus with increasing confining pressure. Thus, the dependency of resilient modulus on both stress controls was assessed.

To ease this process, the 16 loading sequences defined in NCHRP 1-28 A (see Table 4.4) were organized into groupings based on the variation of confining pressure and deviator stress. The sequence groupings used to analyze the resilient modulus

data according to variations in confining pressure are shown in Table 5.8. The 16 load cycles were grouped into a second arrangement and used to analyze the resilient modulus data according to variations in octahedral shear (i.e. deviator) stress. These groupings are summarized in Table 5.9. In groupings 1 through 4, deviator stress is held constant and confining pressure is varied. In groupings 5 through 8, confining pressure is held constant and deviator stress is varied.

Plots of resilient modulus versus bulk stress for grouping 3 (sequences 9 through 12) are shown for samples $B1_N$, $D1_N$, and $E1_N$ in Figure 5.7. Plots of resilient modulus versus octahedral shear stress for grouping 5 (sequences 1, 5, 9, and 13) are shown for $B1_N$, $D1_N$, and $E1_N$ in Figure 5.8. Three specimens were tested for each gradation shown. Resilient modulus for a single gradation is reported as the average resilient modulus of the three specimens tested for that gradation.

As expected, resilient modulus of RAS increased with increasing bulk stress. For the range of bulk stresses studied, specimen $D1_N$ exhibited the highest resilient modulus of the three RAS gradations. Resilient modulus of $D1_N$ was 34 MPa for a bulk stress of approximately 120 kPa (equivalent to a confining pressure of 14 kPa, and deviator stress between 70 and 80 kPa), and 68 MPa for a bulk stress of 260 kPa (equivalent to a confining pressure of 55 kPa, and deviator stress between 70 and 80 kPa). Specimen $B1_N$ exhibited the lowest resilient modulus of the three RAS gradations. Resilient modulus of $B1_N$ was 26 MPa for a bulk stress of 120 kPa, and 50 MPa for a bulk stress of 260 kPa.

Table 5.8 Sequence groupings for analysis of resilient modulus with increasing bulk stress

Grouping	Sequence	Confining Pressure (kPa)	Contact Stress (kPa)	Cyclic Stress (kPa)	Deviator Stress (kPa)	Bulk Stress (kPa)	Octahedral Shear Stress (kPa)	Number Of Repetitions
1	1	55.2	11	27.6	38.6	204.2	18.2	100
	2	41.4	8.3	27.6	35.9	160.1	16.9	100
	3	27.6	5.5	27.6	33.1	115.9	15.6	100
	4	13.8	2.8	27.6	30.4	71.8	14.3	100
2	5	55.2	11	48.3	59.3	224.9	28.0	100
	6	41.4	8.3	48.3	56.6	180.8	26.7	100
	7	27.6	5.5	48.3	53.8	136.6	25	100
	8	13.8	2.8	48.3	51.1	92.5	24.1	100
3	9	55.2	11	69	80	245.6	37.7	100
	10	41.4	8.3	69	77.3	201.5	36.4	100
	11	27.6	5.5	69	74.5	157.3	35.1	100
	12	13.8	2.8	69	71.8	113.2	33.8	100
4	13	55.2	11	96.6	107.6	273.2	50.7	100
	14	41.4	8.3	96.6	104.9	229.1	410	100
	15	27.6	5.5	96.6	102.1	184.9	48.1	100
	16	13.8	2.8	96.6	99.4	140.8	46.9	100

Table 5.9 Sequence groupings for analysis of resilient modulus with increasing octahedral shear stress

Grouping	Sequence	Confining Pressure (kPa)	Contact Stress (kPa)	Cyclic Stress (kPa)	Deviator Stress (kPa)	Bulk Stress (kPa)	Octahedral Shear Stress (kPa)	Number Of Repetitions
5	1	55.2	11	27.6	38.6	204.2	18.2	100
	5	55.2	11	48.3	59.3	224.9	28.0	100
	9	55.2	11	69	80	245.6	37.7	100
	13	55.2	11	96.6	107.6	273.2	50.7	100
6	2	41.4	8.3	27.6	35.9	160.1	16.9	100
	6	41.4	8.3	48.3	56.6	180.8	26.7	100
	10	41.4	8.3	69	77.3	201.5	36.4	100
	14	41.4	8.3	96.6	104.9	229.1	410	100
7	3	27.6	5.5	27.6	33.1	115.9	15.6	100
	7	27.6	5.5	48.3	53.8	136.6	25	100
	11	27.6	5.5	69	74.5	157.3	35.1	100
	15	27.6	5.5	96.6	102.1	184.9	48.1	100
8	4	13.8	2.8	27.6	30.4	71.8	14.3	100
	8	13.8	2.8	48.3	51.1	92.5	24.1	100
	12	13.8	2.8	69	71.8	113.2	33.8	100
	16	13.8	2.8	96.6	99.4	140.8	46.9	100

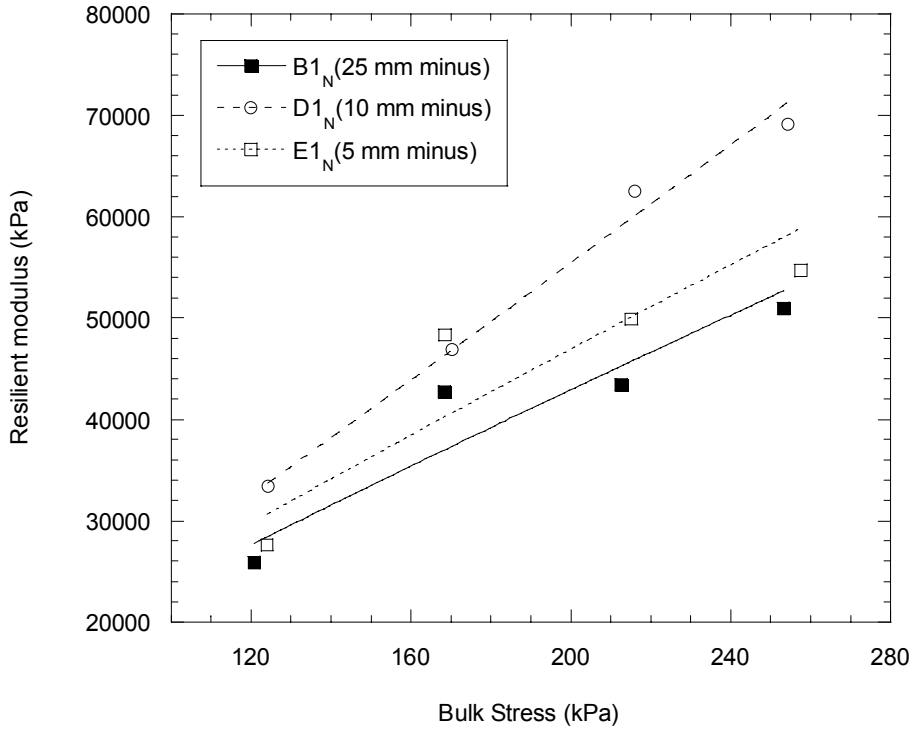

Figure 5.7 Resilient modulus versus bulk stress for 3 RAS gradations

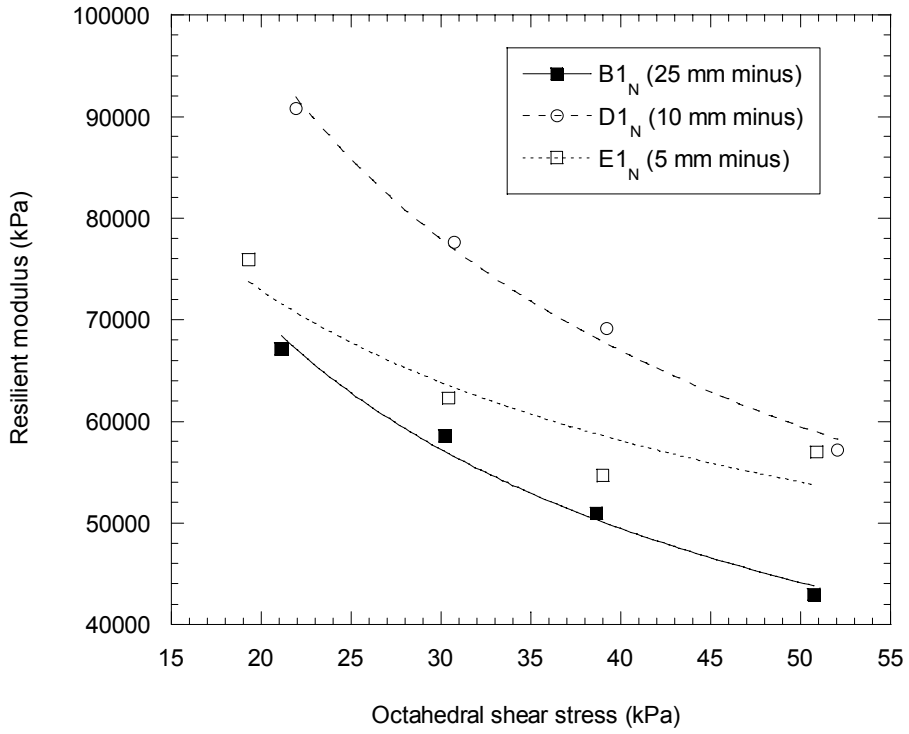

Figure 5.8 Resilient modulus versus octahedral shear stress for 3 RAS gradations

Resilient modulus of RAS decreased with decreasing octahedral shear stress. Again, specimen $D1_N$ exhibited the highest resilient modulus of the three RAS gradations. Resilient modulus of $D1_N$ was 90 MPa for an octahedral shear stress of 22 kPa (equivalent to a confining pressure of 55 kPa, and deviator stress of 39 kPa), and 60 MPa for an octahedral shear stress of 52 kPa (equivalent to a confining pressure of 55 kPa, and deviator stress of 39 kPa). Specimen $B1_N$ exhibited the lowest resilient modulus of the three RAS gradations. Resilient modulus of $B1_N$ was 68 MPa for an octahedral shear stress of 22 kPa, and 44 MPa for a bulk stress of 52 kPa.

. Andrei et al. (2004) suggested that a deviator stress of 41 kPa, and a confining pressure of 14 kPa exemplify the typical stress state experienced by cohesive subgrades in flexible pavement systems. Additionally, the NCHRP 1-28 A protocol suggested that a deviator stress of 103 kPa, and a confining pressure of 35 kPa exemplify the typical stress state experienced by aggregate base course in flexible pavement systems. Resilient moduli of $B1_N$, $D1_N$, and $E1_N$ were calculated for the stress states recommended by Andrei et al. and the NCHRP using the NCHRP 1-28 A revised power model (Eq. 2.2). The results are summarized in Table 5.10. For the stress state outlined by Andrei et al., resilient modulus of RAS ranged from 29 MPa for $B1_N$ to 37 MPa for $D1_N$. For the stress state outlined by the NCHRP, resilient modulus of RAS ranged from 34 MPA for $B1_N$ to 41 MPa for $D1_N$. The empirical parameters (k_1, k_2, k_3, k_6, and k_7) used to model resilient modulus of $B1_N$, $D1_N$, and $E1_N$ according to the NCHRP and Andrei et al. are summarized in Table 5.11.

Table 5.10 Resilient modulus of RAS according to NCHRP 1-28 A power model

Sample ID	RAS Gradation (mm minus)	Mean Resilient Modulus[1] (As Subgrade) (MPa)	C.O.V (%)[3] / Standard Deviation	Mean Resilient Modulus[2] (As Base-subbase) (MPa)	C.O.V. (%)[3] / Standard Deviation
$B1_N$	25	29	9.3 / 2.7	34	4.7 / 1.6
$D1_N$	10	36	14.2 / 5.1	41	9.0 / 3.7
$E1_N$	5	33	8.8 / 2.9	38	1.8 / 0.7

[1]Resilient modulus was calculated using θ = 83 kPa, and τ_{oct} = 19.3 kPa (Andrei et al., 2004)
[2]Resilient modulus was calculated using θ = 208 kPa, and τ_{oct} = 48.6 kPa (NCHRP, 2004)
[3]C.O.V. = coefficient of variance = (standard deviation / mean) * 100%

Table 5.11 Empirical parameters for NCHRP 1-28 A model

Sample ID	RAS Gradation (mm minus)	k_1	k_2	k_3	k_6	k_7
$B1_N$	25	530	0.86	-3.42	-5.54	1.4
$D1_N$	10	604	1.3	-3.84	-17.74	1
$E1_N$	5	600	1.12	-3.22	-14.37	1.1

Note: Reported k-values are the mean of the three specimens tested for each gradation

Sample $B1_N$ was mixed with WisDOT Grade 2 granular backfill at a 50:50 mass-to-mass ratio, compacted to 95% of standard dry unit weight, and tested for resilient modulus according to the NCHRP 1-28 A protocol for cohesive subgrades. Pure specimens of Grade 2 granular backfill were also tested for resilient modulus according to the NCHRP 1-28 A protocol for cohesive subgrades. Although both pure Grade 2 granular backfill and the 50:50 $B1_N$:Grade 2 blend were granular materials, they were tested using the cohesive protocol for the purposes of back comparison to unstabilized RAS.

Plots of resilient modulus versus bulk stress for grouping 3 (sequences 9 through 12) are shown for samples $B1_N$, $B2_G$, and $B3_G$ (pure Grade 2 granular backfill) in Figure 5.9. . Plots of resilient modulus versus octahedral shear stress for grouping 5 (sequences 1, 5, 9, and 13) are shown for $B1_N$, $B2_G$, and $B3_G$ in Figure 5.8.

Resilient moduli of $B1_N$, $B2_G$, and $B3_G$ were calculated using the NCHRP 1-28 A revised power model (Eq. 2.2) and the stress states recommended by the NCHRP and Andrei et al. The results are summarized in Table 5.12. A plot of resilient modulus versus RAS content for RAS-Grade 2 granular backfill mixes is shown in Figure 5.8. For the stress state recommended by Andrei et al., resilient modulus of $B1_N$, $B2_G$, and $B3_G$ ranged from 29 MPa for $B1_N$ to 84 MPa for $B3_G$. For the stress state recommended by the NCHRP, resilient modulus of $B1_N$, $B2_G$, and $B3_G$ ranged from 34 MPa for $B1_N$ to 112 MPa for $B3_G$.

NCHRP project 1-37 A recommends 75 MPa as a minimum resilient modulus for functional base course material. Pure RAS gradations did not meet this requirement, however; pure RAS may be suitable as a filter layer between fine-grained subgrades and granular bases or subbases. Pure RAS may also be suitable for use as a general fill or possibly a drainage layer. Low CBR would limit working platform application over

a soft subgrades. Further testing of RAS for shear strength and compressibility would be necessary to determine its feasibility as general fill material.

Pure, unstabilized RAS exhibited resilient moduli significantly lower than WisDOT Grade 2 granular backfill; an aggregate commonly used in base course construction. One-to-one mixes of 25-mm minus RAS and Grade 2 granular backfill exhibited resilient moduli on the lower end of the range specified by the NCHRP. Mixes of RAS and Grade 2 granular backfill composed of at least 50% gravel by mass may be suitable for use in base course, however; mixing Grade 2 granular backfill with RAS reduces resilient modulus proportionally.

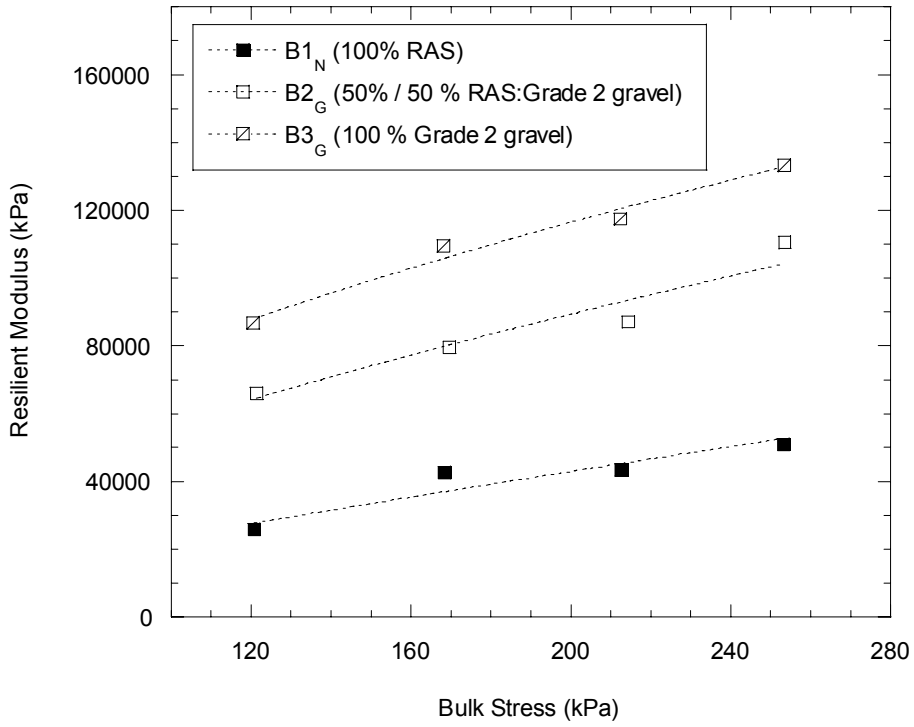

Figure 5.9 Resilient modulus versus bulk stress B series (25-mm minus)

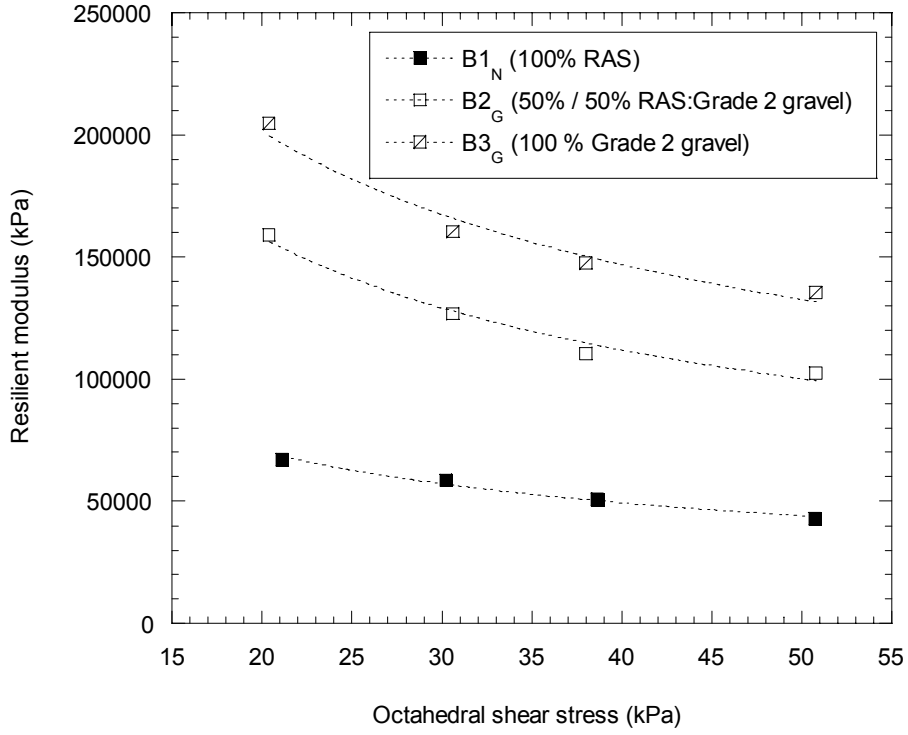

Figure 5.10 Resilient modulus versus octahedral shear stress B series (25-mm minus)

Table 5.12 Resilient modulus of RAS according to NCHRP 1-28 A power model

Sample ID	RAS Gradation (mm minus)	RAS Content (%)	WisDOT Grade 2 Granular Backfill %	Mean Resilient Modulus[1] (As Subgrade) (MPa)	C.O.V (%)[3] / Standard Deviation	Mean Resilient Modulus[2] (As Base-Subbase) (MPa)	C.O.V (%)[3] / Standard Deviation
$B1_N$	25	100	0	29	9.3 / 2.7	34	4.7 / 1.6
$B2_G$	25	50	50	62	4.5 / 2.8	77	3.0 / 2.3
$B3_G$	25	0	100	84	4.9 / 4.1	112	2.7 / 3.0

[1]Resilient modulus was calculated using θ = 83 kPa, and τ_{oct} = 19.3 kPa (Andrei et al., 2004)
[2]Resilient modulus was calculated using θ = 208 kPa, and τ_{oct} = 48.6 kPa (NCHRP, 2004)
[3]C.O.V. = coefficient of variance = (standard deviation / mean) * 100%

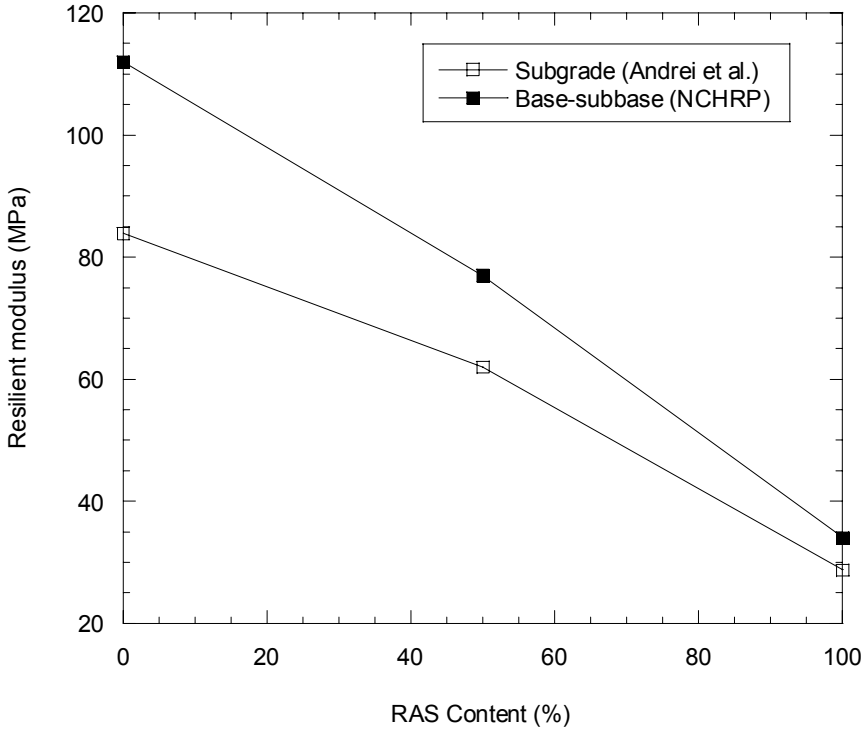

Figure 5.11 Resilient modulus versus RAS content – B series

When a material is exposed to cyclical periods of loading and unloading, (such as in a resilient modulus test) it will exhibit hysteretic behavior i.e. as the applied stress is released, the material will begin to rebound (elastic or recoverable strain), but will not fully rebound to its original dimensions. Permanent deformation (plastic or permanent strain) is not recoverable, and accrues with each additional application of stress to the material. In the field, the continued accruement of plastic strains in base course could cause rutting in the surface pavement. Materials that resist excessive buildup of plastic strains are desirable for base course construction. Total plastic strain and permanent deformation were measured for all specimens at the conclusion of the resilient modulus test and are reported in Table 5.13.

Pure RAS gradations exhibited more permanent deformation and plastic strain than RAS-Grade 2 mixtures and pure Grade 2 granular backfill. Of the pure RAS gradations tested, sample $B1_N$ exhibited the largest permanent deformation and thus, the largest plastic strain. Sample $D1_N$ exhibited the least permanent deformation and plastic strain of the three pure RAS gradations. The permanent deformation of Grade 2 increases with increasing RAS content.

Table 5.13 Total permanent deformation and plastic strain for RAS, and RAS-Grade 2 mixtures

Sample ID	RAS Content (%)	RAS Size (mm minus)	Grade 2 Granular Backfill Content (%)	Mean Total Deformation (mm)	C.O.V. (%)[1] / Standard Deviation	Mean Plastic Strain (%)	C.O.V. (%)[1] / Standard Deviation
$B1_N$	100	25	0	3.2	8.8 / 0.28	1.6	8.4 / 0.14
$B2_G$	50	25	50	1.1	13.9 / 0.15	0.5	15.1 / 0.08
$B3_G$	0	N/A	100	0.5	15.0 / 0.08	0.2	17.6 / 0.04
$D1_N$	100	10	0	1.7	21.2 / 0.36	0.8	18.3 / 0.15
$E1_N$	100	5	0	2.1	9.8 / 0.21	1.1	9.1 / 0.10

[1]C.O.V. = coefficient of variation = (standard deviation / mean) * 100%

5.2 PROPERTIES OF FLY ASH STABILIZED RAS

A primary objective of this study was to determine whether unstabilized RAS was suitable as a replacement for virgin aggregates in base course construction. As evidenced by CBR and resilient modulus tests, unstabilized RAS is unsuitable as base course material. Recent studies have shown that fly ash, a byproduct of coal combustion, can be used as a stabilizer for soft subgrades, weak subbase and base course aggregates, and embankment fills (Senol et al, 2002). Specimens of RAS were stabilized with class C fly ash (20% by dry mass of RAS) from Columbia Power Plant near Portage, WI and tested for compaction, CBR, resilient modulus, and unconfined compressive strength. RAS specimens chosen for fly ash stabilization were $B1_N$ and $D1_N$.

5.2.1 Compaction test results

The compaction characteristics of fly ash stabilized RAS (S-RAS) were measured using standard Proctor compaction effort (ASTM D 698). Compaction curves for S-RAS are shown in Figure 5.12. The maximum dry unit weights and optimum water contents for fly ash stabilized and unstabilized $B1_N$ and $D1_N$ are shown in Table 5.14. The addition of fly ash resulted in an increase in maximum dry unit weight. The maximum dry unit weight of $B1_N$ when stabilized with fly ash was 11.9 kN/m^3; approximately 2 kN/m^3 higher than the unstabilized specimen. The optimum water content for fly ash stabilized B1N was 12%; an increase of 2% from the unstabilized specimen. The maximum dry unit weight of $D1_N$ when stabilized with fly ash was 13.7 kN/m^3; approximately 2 kN/m^3 higher than the unstabilized specimen. The optimum

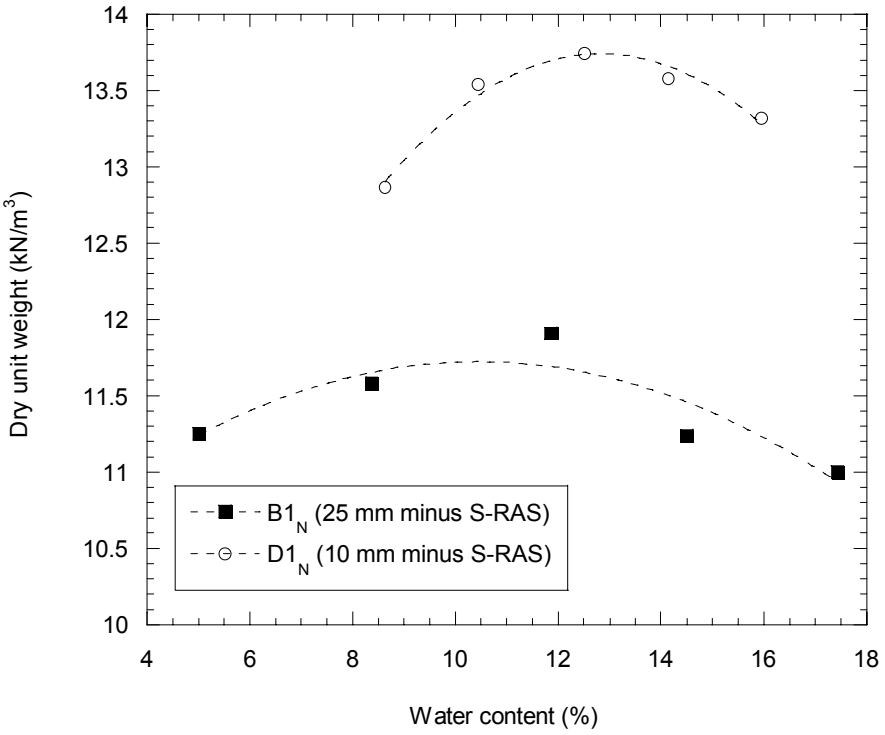

Figure 5.12 Standard Proctor compaction curves for two S-RAS gradations stabilized with 20% class C fly ash

Table 5.14 Compaction test results for S-RAS and unstabilized RAS

Sample ID	RAS Gradation (mm)	Fly Ash Content (%)	Dry Unit Weight (kN/m^3)	Optimum Water Content (%)
$B1_N$ (unstabilized)	25	0	10.4	10
$B1_N$ (S-RAS)	25	20	11.9	12
$D1_N$ (unstabilized)	10	0	12.5	14
$D1_N$ (S-RAS)	10	20	13.7	13

water content for fly ash stabilized B1N was 13%; a decrease of 1% from the unstabilized specimen.

5.2.2 California Bearing Ratio Test Results

Penetrative resistance of S-RAS, compacted to 95% of the standard Proctor maximum dry unit weight and cured for 7 days in a 100% humidity room, was measured using California Bearing Ratio (CBR) tests (ASTM D 1888). The results of these tests are summarized in Table 5.15. Fly ash stabilization of $B1_N$ and $D1_N$ resulted in a two-fold increase in CBR. Even so, S-RAS was deemed unsuitable as subbase or base course material on the basis of CBR parameters outlined in Table 5.6.

As mentioned in section 5.1.3, CBR is only an index property. Further evaluation of resilient modulus and unconfined compressive strength are needed to fully to determine whether S-RAS is capable of supporting overburden and live traffic loads when protected by a surface pavement. However, CBR is a relevant property for working platforms for construction over soft subgrades because a working platform has to support construction traffic without significant rutting (25 mm or more) prior to construction of the pavement structure. In this sense, RAS even after fly ash stabilization appear to be inadequate as a working platform with CBR less than 10.

Table 5.15 CBR of S-RAS and RAS

Sample ID	RAS Gradation (mm)	Fly Ash Content (%)	CBR
$B1_N$ (unstabilized)	25	0	2
$B1_N$ (S-RAS)	25	20	5
$D1_N$ (unstabilized)	10	0	3
$D1_N$ (S-RAS)	10	20	7

Note: S-RAS specimens were cured for 7 days in a 100% humidity room

5.2.3 Resilient modulus test results

Fly ash stabilized RAS specimens ($B1_N$ and $D1_N$) were tested for resilient modulus according to the NCHRP 1-28 A protocol for cohesive subgrades. S-RAS specimens were compacted to a minimum of 95% of the standard Proctor maximum dry unit weight and cured in a 100% humidity room prior to testing. Three specimens were prepared for each gradation. Two sets of three S-RAS specimens were prepared for gradation $D1_N$. One set was cured for 7 days, while the other set was cured for 28 days. This was done to determine the effect of curing length on S-RAS resilient modulus.

Plots of resilient modulus versus bulk stress (sequence grouping 3 from Table 5.8) for S-RAS and unstabilized RAS are shown in Figure 5.10. Plots of resilient modulus versus octahedral shear stress (sequence grouping 5 from Table 5.9) are shown for S-RAS and unstabilized RAS in Figure 5.11. Resilient modulus for a single gradation was calculated as the average of the three specimens tested.

Resilient moduli of S-RAS and RAS were calculated with the NCHRP 1-28 A revised power model (Eq. 2.3) for the stress state recommended Andrei et al. for cohesive subgrades, and for the stress state recommended by the NCHRP for base and subbase course. The results are summarized in Table 5.16. In general, resilient modulus of S-RAS improved over unstabilized specimens, however; the improvement in resilient modulus was not sufficient enough to warrant its use in base course construction.

For the stress state recommended by Andrei et al., resilient modulus of S-RAS ranged from 38 MPa for $B1_N$ (7-day cure) to 60 MPa for $D1_N$ (28-day cure). For the stress state recommended by the NCHRP, resilient modulus of S-RAS ranged from 41 MPa for $B1_N$ (7-day cure) to 62 MPa for $D1_N$ (28-day cure). Resilient modulus of fly ash stabilized $B1_N$ increased by approximately 7 to 9 MPa over unstabilized $B1_N$. Resilient modulus of fly ash stabilized $D1_N$ (7-day cure) increased by approximately 18 MPa over

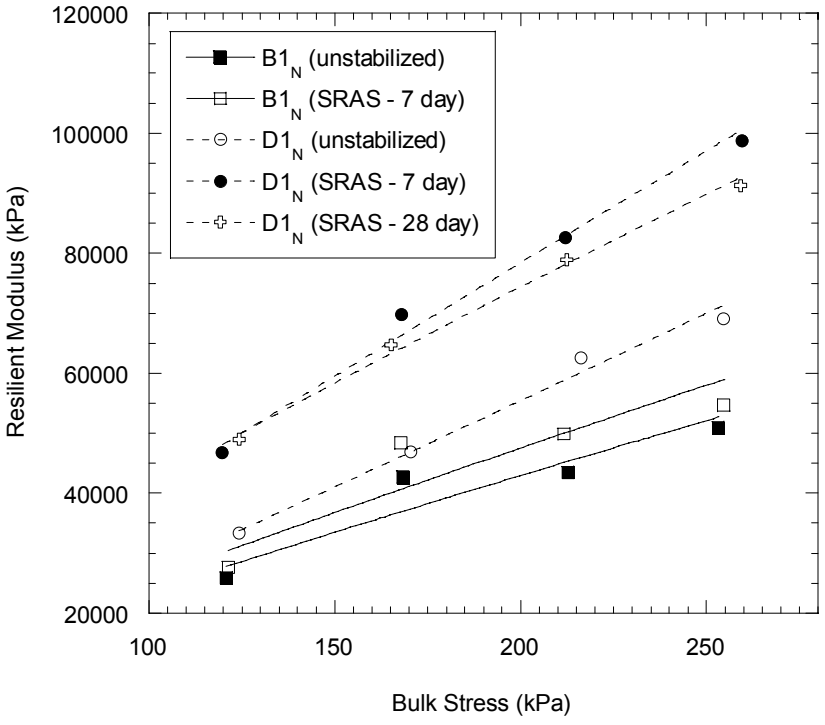

Figure 5.13 Resilient modulus versus bulk stress for S-RAS (7 and 28 day cure) and RAS

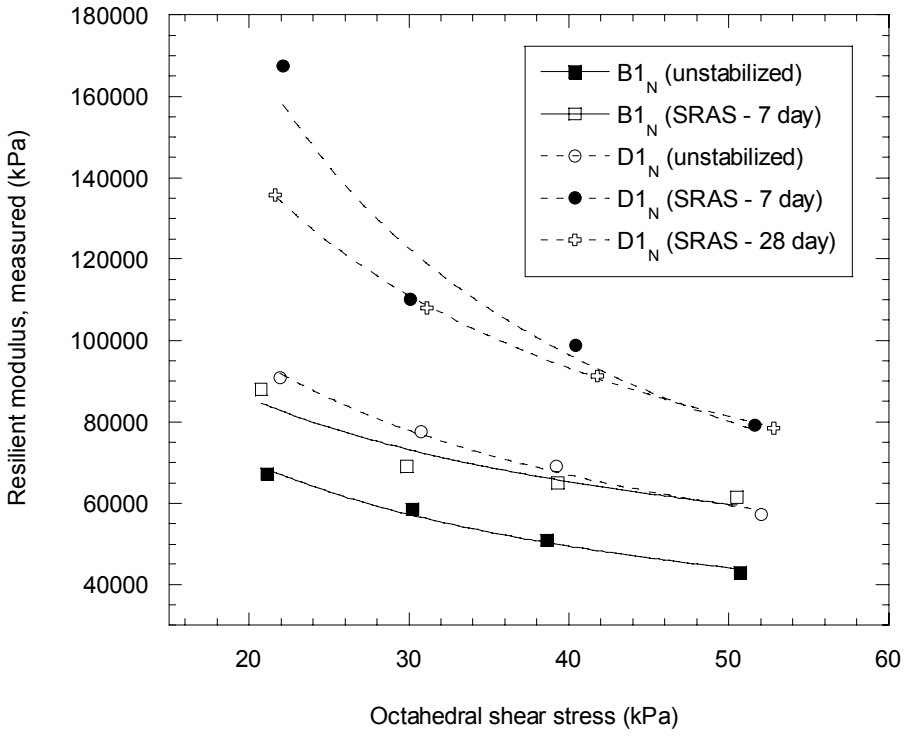

Figure 5.14 Resilient modulus versus octahedral shear stress for S-RAS (7 and 28 day cure) and RAS

Table 5.16 Resilient modulus of S-RAS and RAS according to NCHRP 1-28 A model

Sample ID	RAS Gradation (mm minus)	Fly Ash Content (%)	Curing Time (days)	Mean Resilient Modulus[1] (As Subgrade) (MPa)	C.O.V. (%)[3] / Standard Deviation	Mean Resilient Modulus[2] (As Base-subbase) (MPa)	C.O.V. (%)[3] / Standard Deviation
$B1_N$ (unstabilized)	25	0	0	29	9.3 / 2.7	34	4.7 / 1.6
$B1_N$ (S-RAS 7-day)	25	20	7	38	2.9 / 1.1	41	7.6 / 3.1
$D1_N$ (unstabilized)	10	0	0	36	14.2 / 5.1	41	9.0 / 3.7
$D1_N$ (S-RAS 7-day)	10	20	7	55	5.8 / 3.2	59	2.4 / 1.4
$D1_N$ (S-RAS 28-day)	10	20	28	60	0.8 / 0.5	62	1.0 / 0.6

[1]Resilient modulus was calculated using θ = 83 kPa, and τ_{oct} = 19.3 kPa (Andrei et al., 2004)
[2]Resilient modulus was calculated using θ = 208 kPa, and τ_{oct} = 48.6 kPa (NCHRP, 2004)
[3]C.O.V. = coefficient of variance = standard deviation / mean * 100%

Table 5.17 Empirical parameters for NCHRP 1-28 A power model

Sample ID	RAS Gradation (mm minus)	Fly Ash Content (%)	Curing Period (days)	k_1	k_2	k_3	k_6	k_7
$B1_N$ (unstabilized)	25	0	0	530	0.86	-3.42	-5.54	1.4
$B1_N$ (S-RAS 7-day)	25	20	7	407	1.35	-3.82	-16.81	1
$D1_N$ (unstabilized)	10	0	0	604	1.3	-3.84	-17.74	1
$D1_N$ (SRAS 7-day)	10	20	7	794	1.31	-4.2	-16.45	1
$D1_N$ (SRAS 28 day)	10	20	28	888	1.5	-4.61	-22.02	1

Note: Reported k-values are the mean of the three specimens tested for each gradation

unstabilized $D1_N$. Resilient modulus of 28-day cure $D1_N$ specimens improved by 3 to 4 MPa over 7-day cure specimens. The empirical parameters (k_1, k_2, k_3, k_6, and k_7) used to model resilient modulus of S-RAS (7 and 28-day cure) and unstabilized RAS according to NCHRP 1-28 A are summarized in Table 5.17.

Total plastic strain and permanent deformation were measured for all specimens at the conclusion of resilient modulus testing and are reported in Table 5.18. Pure RAS specimens exhibited more permanent deformation and plastic strain than S-RAS specimens. Of the S-RAS specimens tested, $B1_N$ (7-day cure) exhibited the largest permanent deformation and thus, the largest plastic strain. $D1_N$ (7-day cure) and $D1_N$ (28-day cure) exhibited identical plastic strains. The additional curing length appears to have little effect on the plastic strain experienced by S-RAS specimens during resilient modulus testing.

Table 5.18 Total permanent deformation and plastic strain for RAS, S-RAS (7-day cure) and S-RAS (28-day cure) specimens

Sample ID	RAS Size (mm minus)	Fly Ash Content (%)	Mean Total Deformation (mm)	C.O.V. (%)[1] / Standard Deviation	Mean Plastic Strain (%)	C.O.V. (%)[1] / Standard Deviation
$B1_N$ (unstabilized)	25	0	3.2	8.8 / 0.28	1.6	8.4 / 0.14
$B1_N$ (7-day cure)	25	20	1.1	46.2 / 0.49	0.5	48.1 / 0.26
$D1_N$ (unstabilized)	10	0	1.7	21.2 / 0.36	0.8	18.3 / 0.15
$D1_N$ (7-day cure)	10	20	0.7	14.6 / 0.11	0.4	15.5 / 0.06
$D1_N$ (28-day cure)	10	20	0.7	13.4 / 0.10	0.4	13.6 / 0.05

[1]C.O.V. = coefficient of variation = (standard deviation / mean) * 100%

5.2.4 Unconfined compressive strength test results

Fly ash stabilized RAS specimens were tested for unconfined compressive strength according to ASTM D 2166 after completion of resilient modulus testing. S-RAS specimens were compressed at a rate of 0.21% strain per minute until peak compressive strength was achieved.

The results of unconfined compressive strength testing are summarized in Table 5.19. The unstabilized RAS gradations chosen for unconfined compressive strength testing were defined as coarse, granular materials in Section 5.1.1. Granular materials have minimal compressive strength when unconfined. Thus, the unconfined compressive strength of unstabilized RAS was assumed to be zero. Unconfined compressive strength of fly ash stabilized $B1_N$ (7-day cure) is 212 kPa. Unconfined compressive strength of 28-day cure $D1_N$ increased by 19 kPa over 7-day cure $D1_N$.

Senol et al. (2002) performed unconfined compressive tests on fly ash-stabilized specimens of low-plasticity clay. The CBR of the unstabilized clay was similar to RAS (~1-2). Additionally, the clay was stabilized with Columbia Class C fly ash and cured for 7 days in the same manner as this study. Thus, the study by Senol et al. provides a reasonable comparison of unconfined compressive strength of S-RAS and a fly ash-stabilized soft subgrade.

Senol et al. observed that unconfined compressive strength of fly ash-stabilized clay specimens (20% fly ash by mass) increased by approximately 700 to 1100 kPa over unstabilized specimens. The quantity of improvement observed by Senol et al. is significantly greater than the improvement observed for S-RAS specimens in this study.

The S-RAS does not appear to benefit nearly as much from fly ash stabilization as the soft clays studied by Senol et al. There are several potential explanations for this phenomenon. First, RAS contains significant quantities of asphalt, a highly organic material. Generally, fly ash cements better when mixed with inorganic soils such as

silts, clays, and sands. There is probably diminished pozzolanic activity in stabilized RAS unlike these natural soil materials. Second, the specific gravity and optimum compaction characteristics of RAS are such that the compacted void ratio of RAS is much higher than that of a clay compacted at optimum water content and maximum dry unit weight. As the void ratio increases, the particles become less and less interconnected. The possibility exists that when RAS is mixed with fly ash, the fly ash adheres to and coats the individual particle surfaces, but is unable to adequately bond the RAS particles together because of the decreased interconnectedness between the RAS particles.

Table 5.19 Unconfined compressive strength of S-RAS and RAS

Sample ID	RAS Gradation (mm)	Fly Ash Content (%)	Curing Time (days)	Unconfined Compressive Strength (kPa)
$B1_N$ (unstabilized)	25	0	0	~0
$B1_N$ (S-RAS 7-day)	25	20	7	212
$D1_N$ (unstabilized)	10	0	0	~0
$D1_N$ (S-RAS 7-day)	10	20	7	214
$D1_N$ (S-RAS 28-day)	10	20	28	233

SECTION SIX

CONCLUSIONS

For the purposes of this study, RAS was analyzed as if it were a soil or aggregate. RAS is not a soil or aggregate, thus, some of the assumptions built into the tests used in this study may not be directly applicable to RAS. First and foremost, the basic assumptions built in to the USCS classification system do not fit well with the particulate nature of RAS. In the future, RAS should be classified according to more appropriate parameters such as average particle aspect ratio, asphalt content, relative percentages of plate-like particles, mass ratio of fiberglass to cellulose, etc.

The particle size characteristics of RAS are dependent on the procedure used to manufacture RAS at a recycling facility. Different recycling facilities will undoubtedly use different processing techniques. Additionally, different facilities will produce RAS with varying quantities of tear-off and manufacturer scrap shingles. As such, the particle size and compositional characteristics of RAS are unique to the facility at which it is produced. In the future, it may be beneficial to standardize RAS production and classification procedures.

Large RAS particles are a combination of a cellulose or a fiberglass backing, asphalt coating, imbedded sand grains, and mineral filler. In smaller RAS particles, these constituents are broken down and separated out. As such, the aspect ratio of particle length to thickness decreases proportionally with decreasing RAS particle size. Thus, RAS mixes composed primarily of particles less than 10 mm tend to pack better than RAS composed primarily of particles larger than 10 mm. In any manner, the findings of this study suggest that the packing characteristics of RAS are related to particle size, aspect ratio, and dimensions. Smaller particle size, in general, leads to

higher compaction density; however, nature of RAS also has an impact on compaction density. RAS is not very sensitive to compaction moisture, which is a positive quality.

The localized penetrative resistance, or CBR, of RAS is small for all gradations studied. Penetrative resistance of RAS improves slightly with increasing dry unit weight, however; the improvement is not sufficient to prevent localized penetrative failure of compacted RAS. Due to low CBR, RAS is not suitable as a working platform for construction over soft subgrades.

.According to resilient modulus test results, pure, unstabilized RAS is unsuitable as base material although it can be used as a filter layer between fine-grained subgrades and granular base, i.e., as a subbase course. Additionally, RAS-Grade 2 granular backfill mixtures (minimum 50:50 mass-to-mass ratio) are suitable for use as subbase and are potentially suitable for use as base course in an unstabilized state (resilient modulus ~ 77 MPa). However, resilient modulus of Grade 2 granular backfill decreases proportionally with increasing RAS content.

Fly ash stabilized (class C at 20% by dry mass of RAS) RAS is less susceptible to penetrative deformation than unstabilized RAS, however; S-RAS is still highly susceptible to penetrative deformation when unpaved (i.e., CBR < 10). S-RAS experienced measurable improvement in resilient modulus over unstabilized specimens; however, the improvement does not render S-RAS as a base course material. S-RAS resilient modulus increases with increasing curing time for time periods longer than 7 days, however; overall stiffness gain is small (2-4 MPa).

Fly ash improves RAS to a smaller extent than it does improve low-plasticity clays. This may be due to the high asphalt content of RAS particles and resulting diminishment in pozzolanic activity and/or the diminished particle interconnectedness for cementation.

SECTION SEVEN

PRACTICAL IMPLICATIONS

In light of the resilient modulus, CBR, and unconfined compressive strength test results, RAS and S-RAS are not suitable for use in base course construction. However, RAS and S-RAS may be suitable as a subbase filter layer between fine grained subgrades and granular bases, i.e., as a subbase material. Similarly, RAS and S-RAS may be suitable as general fill material or drainage material. However, Additional studies are necessary to further assess the practicality of using RAS, S-RAS, and RAS composite mixtures as filter, fill or drainage material. Shear strength, hydraulic conductivity, and compressibility studies would be most beneficial for such an evaluation.

S-RAS exhibited marginal improvement in CBR, resilient modulus, and unconfined compressive strength as compared to other soft subgrade materials. For some reason, the waste shingles exhibit decreased pozzolanic and cementation activity as compared to other fly-ash stabilized materials. However, other forms of stabilization i.e. cold asphalt emulsion, etc. might prove more effective in strengthening RAS. Further studies in regards to alternative stabilization methods of RAS would prove whether the beneficial reuse of RAS as base course is indeed possible.

The recycling and reuse of waste materials as replacements for natural materials is a new field of research. In the future, more and more waste materials will be considered for reuse in geotechnical applications. Care must be taken when analyzing the behavior of new materials according to the tests designed for natural earth materials. Additional research of RAS and other potentially recyclable materials can only benefit society in its efforts to promote technically sound, environmentally conservative design initiatives.

SECTION EIGHT

REFERENCES

AASHTO, (1993), Guide for Design of Pavement Structures. American Association of State and Highway and Transportation Officials, Washington D.C., 1993.

Andrei, D., Witczak, M., Schwartz, C., and Uzan, J., (2004) "Harmonized Resilient Modulus Test Method for Unbound Pavement Materials", Transportation Research Record 1874, 2004, pp. 29-37.

Cascadia Consulting Group, (2003), "Wisconsin Statewide Characterization Study", Final Report, 2003.

Crivit, D., (2005), "Overcoming the Barriers to Asphalt Shingle Recycling: Final Report for the RMRC Project 22", Final Report, Research Project RMRC 22, Minnesota Department of Transportation, Minnesota, 2005.

Edil, T., and Bosscher, P., (1994), "Engineering Properties of Tire Chips and Soil Mixtures", Geotechnical Testing Journal, GTJODJ, Vol. 17, No. 4, December 1994, pp. 453-464.

Edil, T., Acosta, H., and Benson, C., (2006) "Stabilizing Soft Fine-Grained Soils with Fly Ash", Journal of Materials in Civil Engineering, ASCE, March 2006, pp. 283-295.

Holtz, R., and Kovacs, W., (1981), Introduction to Geotechnical Engineering. Prentice-Hall, Englewood Cliffs, New Jersey.

Hooper, F., and Marr, W., (2004), "Effects of Reclaimed Asphalt Shingles on Engineering Properties of Soils," *Recycled Materials in Geotechnics*, ASCE Civil Engineering Conference and Exposition, October, 2004, pp. 137-149.

Huang, Y., (1993), Pavement Analysis and Design. Prentice-Hall, Englewood Cliffs, New Jersey.

Jin, M., Lee, K., and Kovacs, W., (1994), "Seasonal Variation of Resilient Modulus of Subgrade Soils", Journal of Geotechnical Engineering, Vol. 120, No. 4, July/August 1994, pp. 603-615.

Koziar, P., Wisconsin Department of Natural Resources, Waste Management Program, Personal Communication, 2005.

Li, D., and Selig, E., (1994), "Resilient Modulus for Fine-Grained Subgrade Soils", Journal of Geotechnical Engineering, Vol. 120, No. 6, June 1994, pp. 939-957.

Marks, V., and Petermier, G., (1997), "Let Me Shingle Your Roadway", Interim Report, Research Project HR-2079, Iowa Department of Transportation, Iowa, 1997.

Mitchell, J., (1993), Fundamentals of Soil Behavior. 2nd ed. John Wiley and Sons, Inc. New York, New York.

Moosazedh, J., and Witczak, M., (1981), "Prediction of Subgrade Moduli for Soil That Exhibits Nonlinear Behavior", Transportation Research Record 810, 1981, pp. 10-17.

Muhanna, A., Rahman, M., and Lambe, P., (1998), "Model for Resilient Modulus and Permanent Strain of Subgrade Soils", Transportation Research Record 1619, 1998, pp. 85-93.

NCHRP, (2004), "Laboratory Determination of Resilient Modulus for Flexible Pavement Design", NCHRP Project 1-28 A, National Cooperative Highway Research Program, January, 2004.

NCHRP (2004), "Guide for Mechanistic-Empirical Design on New and Rehabilitated Pavement Structures", NCHRP Project 1-37 A, National Cooperative Highway Research Program, March, 2004.

Rada, G., and Witczak, M., (1981), "Comprehensive Evaluation of Laboratory Resilient Moduli Results for Granular Material", Transportation Research Record 810, 1981, pp. 22-33.

Seed, H., Chan, C., and Lee, C., (1962), "Resilience Characteristics of Subgrade Soils and their Relation to Fatigue Failures", Proc. Int. Conf. on the Structural Design of Asphalt Pavements, Ann Arbor, Mich., 1962, pp. 611-636.

Senol, A., Bin-Shafique, S., Edil, T., and Benson, C., (2002), "Use of Class C Fly Ash for Stabilization of Soft Subgrade", Fifth International Conference on Advances in Civil Engineering, Istanbul, Turkey, September, 2002.

Shingle Recycling Organization, (2005), "From Roofs to Roads: Recycled Asphalt Roofing Shingles into Paving Materials," Information and Guidance Brochure, www.shinglerecycling.org, 2005.

Thompson, M., and Robnett, Q., (1979), "Resilient Properties of Subgrade Soils", Transportation Engineering Journal of the American Society of Civil Engineers, Proceedings of the American Society of Civil Engineers, Vol. 105, No. TE1, January, 1979, pp. 71-89.

Tian, P., Zaman, M., and Laguros, J., (1998), "Gradation and Moisture Effects on Resilient Moduli of Aggregate Bases", Transportation Research Record 1619, 1998, pp. 75-83.

Wisconsin Department of Transportation, (2007), "Construction and Materials Manual", http://roadwaystandards.dot.wi.gov/standards, Wisconsin Department of Transportation, Wisconsin, 2007.

APPENDIX A

PARTICLE SIZE CURVES FOR GRADE 2 GRANULAR BACKFILL AND BOARDMAN SILT

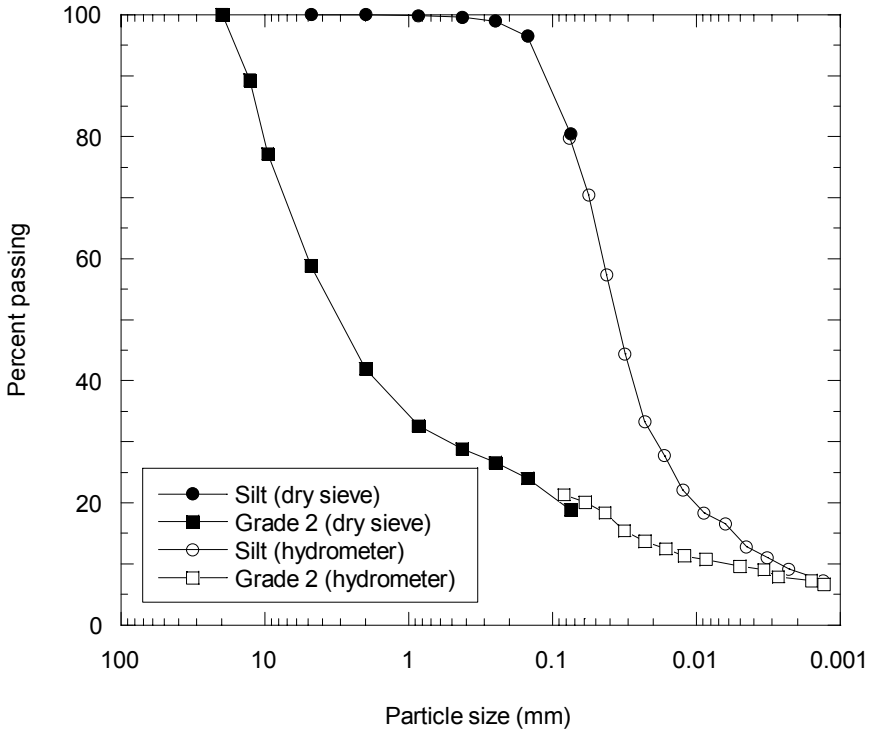

Figure A.1 Particle size curves for Grade 2 granular backfill and Boardman silt

APPENDIX B

RAS PARTICLE SIZE CURVES PRIOR TO AND AFTER COMPACTION

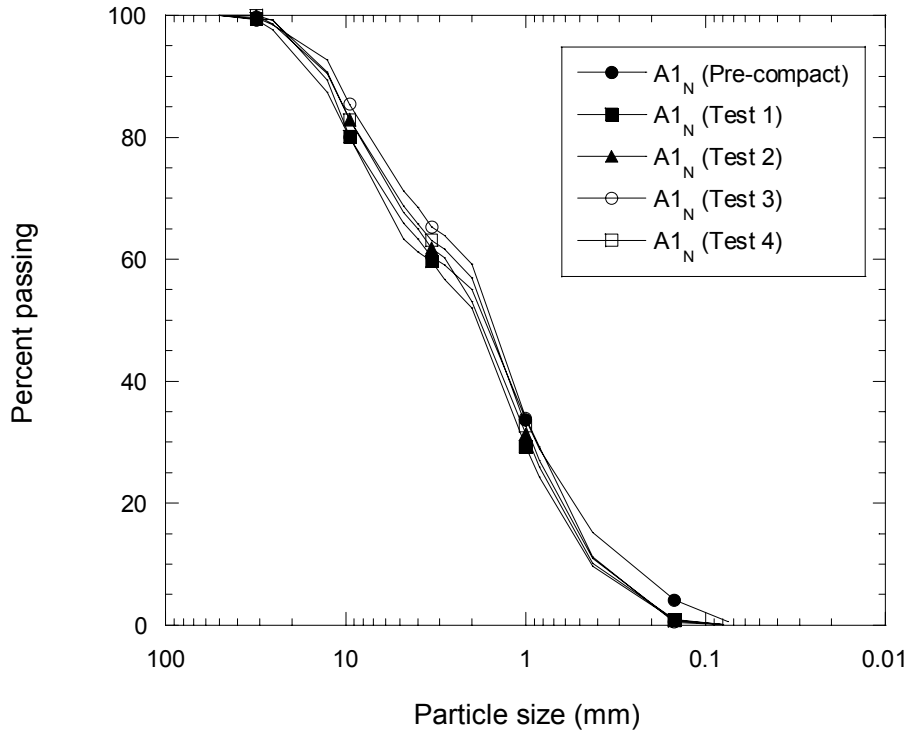

Figure B.1 Particle size curves for $A1_N$ (51-mm minus) prior to and after compaction

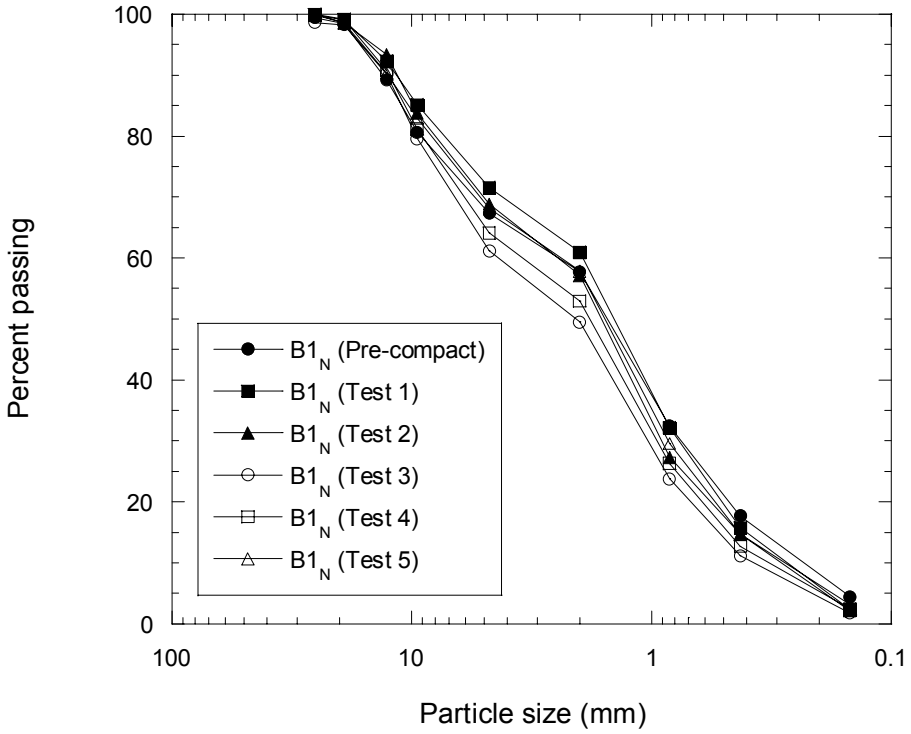

Figure B.2 Particle size curves for $B1_N$ (25-mm minus) prior to and after compaction

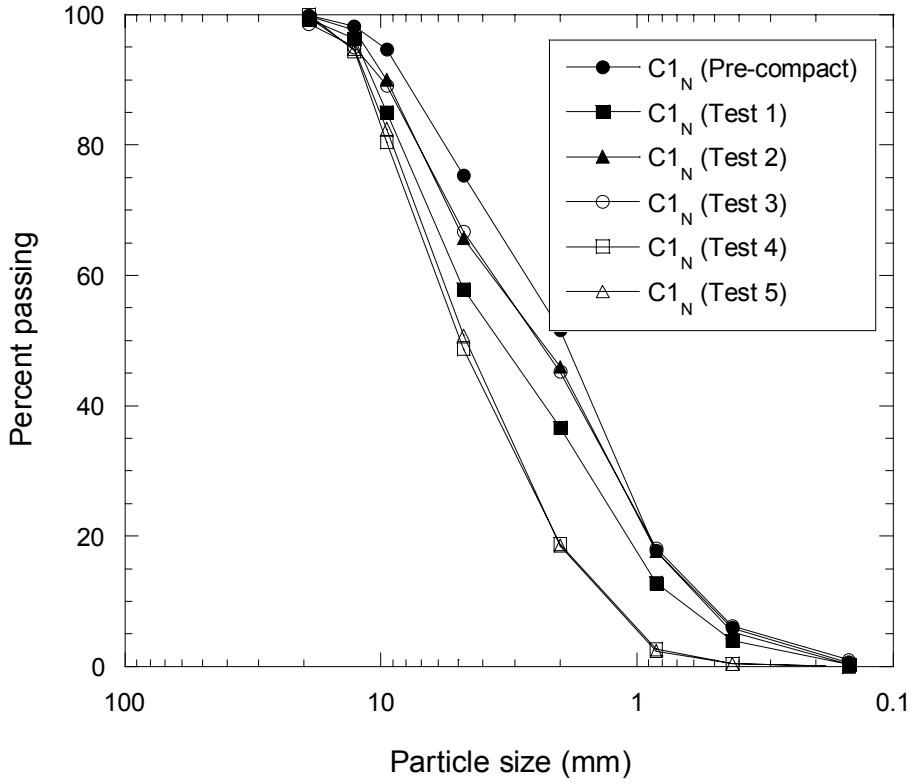

Figure B.3 Particle size curves for $C1_N$ (19-mm minus) prior to and after compaction

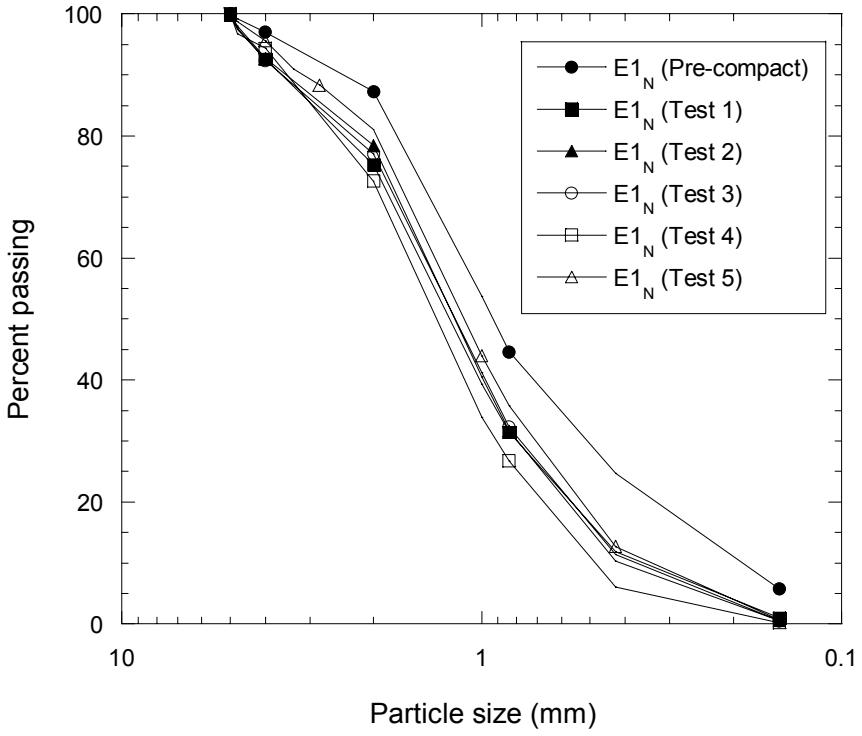

Figure B.4 Particle size curves for $E1_N$ (5-mm minus) prior to and after compaction